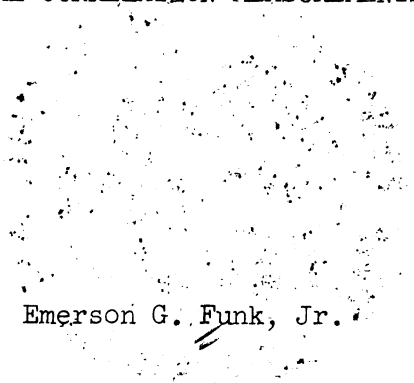THE UNIVERSITY OF MICHIGAN

INDUSTRY PROGRAM OF THE COLLEGE OF ENGINEERING

GAMMA-GAMMA DIRECTIONAL CORRELATION MEASUREMENTS IN Se^{76} AND Cd^{110}

Emerson G. Funk, Jr.

A dissertation submitted in partial fulfillment
of the requirements for the degree of
Doctor of Philosophy in the
University of Michigan
1958

March, 1958

IP-272

Doctoral Committee:

      Professor Marcellus L. Wiedenbeck, Chairman
      Professor H. Richard Crane
      Assistant Professor Karl T. Hecht
      Professor Wilfred Kaplan
      Associate Professor Robert W. Pidd

ACKNOWLEDGMENTS

TABLE OF CONTENTS

LIST OF TABLES

LIST OF FIGURES

LIST OF FIGURES CONT'D

CHAPTER I

INTRODUCTION AND THEORY

Angular Correlation

The main concern of low energy nuclear physics is the determination of the properties of nuclear energy levels and the interpretation of these properties on the basis of nuclear models. Nuclear levels are characterized by their energy, angular momentum (spin), parity, magnetic moment, electric quadrupole moment, and lifetime. The angular correlation of successive nuclear radiations is a very useful method for determining the spin and parity of excited levels and the angular momentum of the emitted radiation. In some cases one can also use angular correlation methods to determine some of the electric and magnetic properties of the nucleus by studying the electric and magnetic interactions of the nucleus with its surrounding fields.

In general the probability of emission of a particle or quantum by a radioactive nucleus depends on the angle between the direction of emission and the nuclear spin axis. Normally, however, the radiation pattern from a radioactive sample is isotropic because the nuclei are randomly oriented in space. Only if the nuclei are aligned by external fields can an anisotropic pattern be expected.

In the case where the nuclei emit two successive radiations an effective alignment can be obtained. This comes about in the following manner. The observation of the first radiation in a given direction selects an ensemble of nuclei that has an anisotropic distribution of spin orientations. The direction of the succeeding radiation then shows

a definite angular correlation with respect to the direction of the first radiation (except in rare cases where isotropy results as an accident[1]).

An angular correlation measurement thus consists of measuring the number of coincidences between the two radiations as a function of the angle subtended by the axes of the two detectors. Actually the term angular correlation comprises both directional correlation and polarization correlation. In a directional correlation, only the directions of the two radiations are observed while in a polarization correlation, the polarization of one or both of the radiations is also measured.

There are many types of correlation processes. The most widely measured types are gamma-gamma[2], beta-gamma[3], alpha-gamma[4], and internal conversion electron-gamma[5] correlations. The information which can be obtained from the correlation depends on the radiations observed and the properties which are singled out by the experiment. Alpha-gamma and gamma-gamma directional correlations yield the spins of the nuclear levels but not the parities. However, the relative parities can be determined if one also observes the polarization of the gamma rays or if one measures the directional correlation between conversion electrons. The directional correlation of a beta-gamma cascade depends on the nuclear spins, the beta energy, the atomic number Z, and the type of interaction involved in the beta decay.

It was first suggested by Pryce in a private communication to Dunworth[6] in 1940 that two successive nuclear radiations will in general be correlated in their relative propagation directions. Independently, Hamilton[7] in 1940 carried out calculations for the gamma-gamma

directional correlation in pure-multipole cascades. Many unsuccessful experimental attempts were made to verify Hamilton's theory in the succeeding years. In 1946, Goertzel[8] investigated the effect of extranuclear fields on a directional correlation. His results explained why some of the experiments disagreed with Hamilton's theory. However, the disagreement of theory and experiment actually was the result of inadequate experimental techniques. In 1947, Brady and Deutsch[9] carried out the first successful correlation measurements using Geiger counters as gamma detectors. The introduction of the scintillation counter as a gamma detector in 1948[10] started a rapid development in the field of angular correlation, and today angular correlation is an important tool in nuclear spectroscopy.

This investigation is concerned with the application of gamma-gamma directional correlation techniques in studying the gamma ray cascades following the beta decay of As^{76} and Ag^{110m}, thus providing information on the spins of the excited states of Se^{76} and Cd^{110}. Three gamma-gamma directional correlations are measured in Se^{76} with the result that unique spin assignments can be made to all of the Se^{76} energy levels. An interpretation of the level scheme in terms of vibrational levels is also made. Six correlations are measured in the complex scheme of Cd^{110} and assignments made to six levels. The results indicate that the sequence of emission of two of the transitions should be the reverse of the order previously reported, thereby changing the level scheme of Cd^{110}. A new level scheme is proposed.

Simplified Theory of Gamma-Gamma Directional Correlation

The general theory of angular correlation has been treated from several different approaches and by numerous authors[7,8,11-20]. The approach which will be presented here is a simplified theory of gamma-gamma directional correlation which provides some physical insight into the problem[21-23].

Consider first a single gamma transition of angular momentum $\vec{L}$ occurring between two nuclear states B and C whose spins are denoted by J_b and J_c respectively. Let L_z be the projection of $\vec{L}$ on the quantization axis (z-axis). The gamma ray is then characterized by the angular momentum quantum number or multipolarity L and the magnetic quantum number M where $L^2 = \hbar^2 L(L+1)$ and $L_z = M\hbar$. The states B and C are described by the quantum numbers J_b, m_b and J_c, m_c where $M = m_b - m_c$.

Each component between two specific magnetic substates has a characteristic directional distribution $F_L^M(\theta)$ where θ denotes the angle between the emitted gamma ray and the z-axis. The angular distribution function $F_L^M(\theta)$ can be found by calculating the Poynting vector as a function of angle for multipole radiation of order L and magnetic quantum number M. It is impossible to separate the individual components $m_b \rightarrow m_c$, and thus the unresolved line $B \rightarrow C$ is always observed. To calculate the total directional distribution $\Omega_L(\theta)$ for the transition $B \rightarrow C$ one must also know the relative population P (m_b) for each substate m_b and the relative transition probability G $(m_b \; m_c)$ for each component $m_b \rightarrow m_c$. The expression for the directional distribution is

then

$$\Omega_L(\theta) \sim \sum_{m_b m_c} P(m_b)\, G(m_b\, m_c)\, F_L^M(\theta) \tag{1}$$

The relative transition probability $G\,(m_b\, m_c)$ depends only on m_b and m_c and not on the specific nuclear properties. It does not depend on the wave functions describing the nuclear states. It can be shown by group theoretical methods[25,26] that $G\,(m_b\, m_c)$ is equal to the square of the Clebsch-Gordan coefficient for the vector addition $\vec{J_b} = \vec{J_c} + \vec{L}$, $m_b = m_c + M$.

$$G(m_b\, m_c) = (J_c\, L\, m_c\, M \mid J_b\, m_b)^2 \tag{2}$$

The relative populations $P\,(m_b)$ depend on the energies of the various m_b states and on the way in which level B was created.

Consider now a nucleus decaying through the cascade $A \rightarrow B \rightarrow C$ by successive emission of two gamma rays. The directional correlation function $W(\theta)$ is the relative probability that γ_1 is emitted at an angle θ with the direction of γ_2. If the quantization axis z is made to coincide with the direction of emission of γ_1, the directional correlation between the two gamma rays becomes the same as $\Omega_{L_2}(\theta)$, the directional distribution of γ_2 with respect to the z-axis. If the relative populations $P(m_b)$ are known, $W(\theta)$ can be calculated from equations (1) and (2). The relative population $P(m_b)$ is given by the sum of all transitions $m_a \rightarrow m_b$ leading into the state m_b. If all m_a states are assumed to be equally populated, then
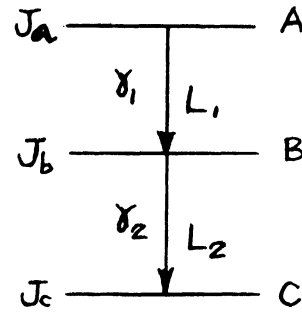
$$P(m_b) \sim \sum_{m_a} G(m_a\, m_b)\, F_{L_1}^{M_1}(o) \tag{3}$$

The special choice of the z-axis makes possible another simplification since a photon moving in a definite direction can have only the angular momentum $\pm\hbar$ along its propagation direction[27]. Therefore M_1 is restricted to the values ± 1 and only the functions $F_{L_1}^{1}(0)$ and $F_{L_1}^{-1}(0)$ appear in equation (3).

The directional correlation function is obtained from equations (1), (2), and (3) and the fact that $W(\theta)=\Omega_{L_2}(\theta)$, giving

$$W(\theta) \sim \sum_{\substack{m_a, m_b, \\ m_c}} (J_b L_1 m_b \pm 1 | J_a m_a)^2 F_{L_1}^{\pm 1}(0) \cdot (J_c L_2 m_c M_2 | J_b m_b)^2 F_{L_2}^{M_2}(\theta) \qquad (4)$$

with $M_2 = m_b - m_c$.

The directional distribution functions $F_L^{M}(\theta)$ can be expressed in powers of $\cos^2\theta$. Therefore $W(\theta)$ is a function of powers of $\cos^2\theta$.

From equation (4) it is seen that the gamma-gamma directional correlation function depends on five parameters, the spins of the three levels and the multipolarity of the two gamma transitions. Therefore information can be gained about these quantities in a directional correlation measurement. However, additional information must be known about some of these quantities if an unambiguous assignment is to be made from a directional correlation measurement.

The directional correlation function does not depend on the parities of the states. This can be understood classically. Electric and magnetic radiations of the same multipole order are related by the transformation $\vec{E} \to \vec{H}, \vec{H} \to -\vec{E}$ [28]. Since the Poynting vector is unaffected by this transformation the directional distributions $F_L^{M}(\theta)$

are not changed and $W(\theta)$ is left unaltered. Thus electric and magnetic
radiation cannot be distinguished in a gamma-gamma directional correlation
measurement, and no information can be gained concerning the parity of
the nuclear states.

Two important assumptions were made in the derivation of the
correlation function.

First, the magnetic sublevels of the initial and final nuclear
states were assumed to be uniformly populated. In practice this condi-
tion is satisfied except when the source is in a strong magnetic field
at very low temperatures, in which case the substates are populated
according to a Maxwell-Boltzmann distribution.

Second, the intermediate state was assumed not to be disturbed
by extranuclear fields[29-32], that is, the sublevels of the intermediate
state should not be repopulated during the lifetime of the state. When
the first gamma ray is detected some knowledge is gained about the ori-
entation of the nucleus from which it came. If the nucleus is affected
by extranuclear fields, it may precess and change magnetic sublevels
before the second gamma ray is emitted. The information gained by the
first detector will then be partially lost and the correlation will be
attenuated. If the maximum correlation is to be attained, the lifetime
of the intermediate state must be short enough so that the fields will
not affect the nucleus before the second gamma ray is emitted. In general,
a lifetime less than 10^{-11} sec. is sufficient to insure this. For states
with longer lifetimes, perturbations are possible, and in order to observe
the maximum correlation one must find a nuclear environment where the

extranuclear fields are small (e.g., a regular lattice site in a cubic crystal) or where their time average vanishes (e.g., certain liquids).

The evaluation of equation (4) for various spins and multipole orders is difficult due to the tedious sums over magnetic quantum numbers. This difficulty was overcome in the general development of the theory. The theory was also extended to include mixed multipole gamma transitions, radiations other than gamma rays, and cases where the intermediate state is perturbed.

Theoretical Results for Gamma-Gamma Directional Correlations

The results of the general theory of angular correlation as applied to gamma-gamma directional correlations will be presented in this section. The results will be put in the notation of Ferentz and Rosenzweig[33].

Pure Gamma-Gamma Cascade

Consider a cascade $j_1 \overset{L_1}{\to} j \overset{L_2}{\to} j_2$. The directional correlation function can be written in the form

$$W(\theta) = \sum_{\substack{k=0 \\ (k\,even)}}^{k_{max}} A_k P_k (\cos\theta) \tag{5}$$

where P_k is the Legendre polynomial of order k. The sum extends only over the Legendre polynomials of even k, and the value of k_{max} is given by the minimum of the set of numbers $(2L_1, 2L_2, 2j)$. Normally one never encounters a k_{max} greater than 4 so that the maximum number of terms needed in the expansion is three. The coefficients A_k can be broken up into two factors, each of which depends on only one step of the cascade.

$$A_k = A_k^{(1)} \cdot A_k^{(2)} \qquad (6)$$

where $\qquad A_k^{(1)} = F_k(L_1\ L_1\ j_1\ j)$

$$A_k^{(2)} = F_k(L_2\ L_2\ j_2\ j) \qquad (7)$$

The F coefficients have been tabulated by Ferentz and Rosenzweig[33] for all conceivable values of the parameters j_1, j_2, j, L_1, and L_2.

Gamma-Gamma Cascade with Mixtures

A gamma transition is said to be of mixed multipolarity when it must be described by more than one value of angular momentum L. Generally the transition probability for magnetic radiation of order L is greater than that for electric radiation of order L + 1, but depending on the energy of the transition, M-L and E-L+1 radiation can compete with each other. A few cases of mixtures between E-L and M-L+1 radiation have also been reported. These are unusual because the transition probability for magnetic radiation of order L+1 is generally much smaller than that for electric radiation of order L. When either or both transitions of a cascade are mixed, the correlation function becomes a coherent sum and cross terms appear.

For a mixed transition, the mixing parameter δ is defined by Biedenharn and Rose[34] as the ratio of the reduced matrix elements for L+1 and L radiation respectively, and it is a real quantity. δ^2 is then the ratio of the total intensity of the L+1 radiation to that of the L

radiation. δ can be either positive or negative depending on the rela-
tive phase of the reduced matrix elements. Lloyd[18] has shown that
only the relative phases 0 and π are of physical significance.

For the case where both transitions of the cascade are mixed
and described by mixing ratios δ_1 and δ_2 respectively, the correlation
function is given by equations (5) and (6) but with $A_k^{(1)}$ and $A_k^{(2)}$
defined as

$$A_k^{(1)} = F_k(L_1 L_1 j_1 j) + 2\delta_1 F_k(L_1 L_1 + 1 \; j_1 j) + \delta_1^2 F_k(L_1 + 1, L_1 + 1, j_1 j) \qquad (8)$$

$$A_k^{(2)} = F_k(L_2 L_2 j_2 j) + 2\delta_2 F_k(L_2 L_2 + 1 \; j_2 j) + \delta_2^2 F_k(L_2 + 1, L_2 + 1, j_2 j) \qquad (9)$$

In even-even nuclei double mixtures are not encountered very frequently,
but in odd A nuclei they occur quite frequently. Since the correlation
function contains two additional parameters in the case of a double mix-
ture the interpretation of correlations is further complicated. Any
experimental correlation function can be explained by many different
spin sequences if double mixtures are considered.

If a mixture occurs in the first transition only, δ_2 can be
set equal to zero, or if a mixture occurs in the second transition only,
δ_1 can be set equal to zero in equations (8) and (9).

Consider the case of a mixture of dipole (L = 1) and quadrupole
(L = 2) radiation occurring in the first transition of a gamma-gamma cas-
cade. Making use of equations (8) and (9) and some of the properties of
the F coefficients, the expansion coefficients A_k can be written as

$$A_0 = 1 , \qquad A_2 = \frac{a + b\delta + c\delta^2}{1 + \delta^2} , \qquad A_4 = \frac{d\delta^2}{1 + \delta^2} \qquad (10)$$

where a,b,c, and d are products of the appropriate F functions for the cascade. To compare the experimental values of A_2 and A_4 with theory one normally plots the quadratic functions given by equations (10) versus δ, but to cover the entire range of δ one must plot δ from 0 to ∞.

For dipole-quadrupole mixtures and especially for large values of δ it is more convenient to introduce the quantity Q where Q is defined as $Q = \delta^2/(1 + \delta^2)$. It is easily seen that Q is the quadrupole content of the radiation while 1-Q is the dipole content. In terms of Q, equations (10) become

$$A_0 = 1, \quad A_2 = a(1-Q) + b\sqrt{Q(1-Q)} + cQ, \quad A_4 = dQ \tag{11}$$

The equation for A_2 is then an ellipse when plotted as a function of Q, and the equation for A_4 is a straight line. Now one need only plot A_2 and A_4 versus Q for values of Q between 0 and 1 to compare the experimental coefficients with the theoretical coefficients.

The 1 -- 3 Directional Correlation

In many nuclear decay schemes more than two gamma rays are in cascade. For example, for a triple cascade one can observe the correlation functions $W(\gamma_1 \gamma_2)$, $W(\gamma_2 \gamma_3)$, and $W(\gamma_1 \gamma_3)$ with the unmentioned radiation being unobserved in each case. The cases of $W(\gamma_1 \gamma_2)$ and $W(\gamma_2 \gamma_3)$ are covered by the previous discussion for a simple double cascade. Biedenharn, Arfken, and Rose[34,35] have extended the theory of angular correlation to the case of the 1 - 3 correlation with the intermediate radiation unobserved.
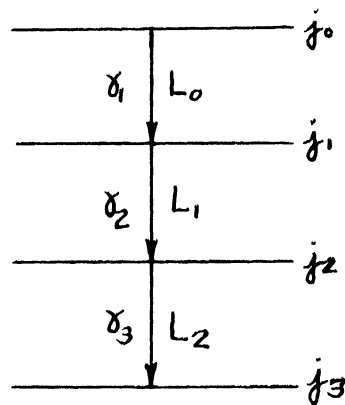
For pure transitions the 1-3 directional correlation function
is given by

$$W(\theta) = (-1)^{L_1-j_1-j_2}\left[(2j_1+1)(2j_2+1)\right]^{\frac{1}{2}}\sum_{k=0}^{k_{max}} F_k(L_0 L_0 j_0 j_1) \cdot$$
$$F_k(L_2 L_2 j_3 j_2) W(j_1 j_1 j_2 j_2; k L_1) P_k(\cos\theta) \tag{12}$$

where $W(j_1\, j_1\, j_2\, j_2;\, k\, L_1)$ is a Racah W-function[15] and k_{max} is given
by the minimum of the set of numbers $(2L_0,\, 2L_2,\, 2j_1,\, 2j_2)$.

If the unobserved transition is mixed, the expression for the
correlation function becomes

$$W(\theta) = W(L_1) + \delta^2\, W(L_1') \tag{13}$$

where $W(L_1)$ and $W(L_1')$ are given by equation (12). The interference
term is not present in this case because the mixed radiation is unob-
served.

If a mixture occurs in the first transition, the correlation
function is given by

$$W(\theta) = W(L_0) + \delta^2 W(L_0') + 2\delta W(L_0 L_0') \tag{14}$$

where $W(L_0)$, $W(L_0')$, and $W(L_0\, L_0')$ are obtained from equation (12).

CHAPTER II

EXPERIMENTAL PROBLEMS

Method

Before going into the experimental problems involved in a

directional correlation measurement the method of making the measurement

will be briefly described. One detector is fixed in position while the

other is free to rotate about the centrally mounted source. (Figure 1)
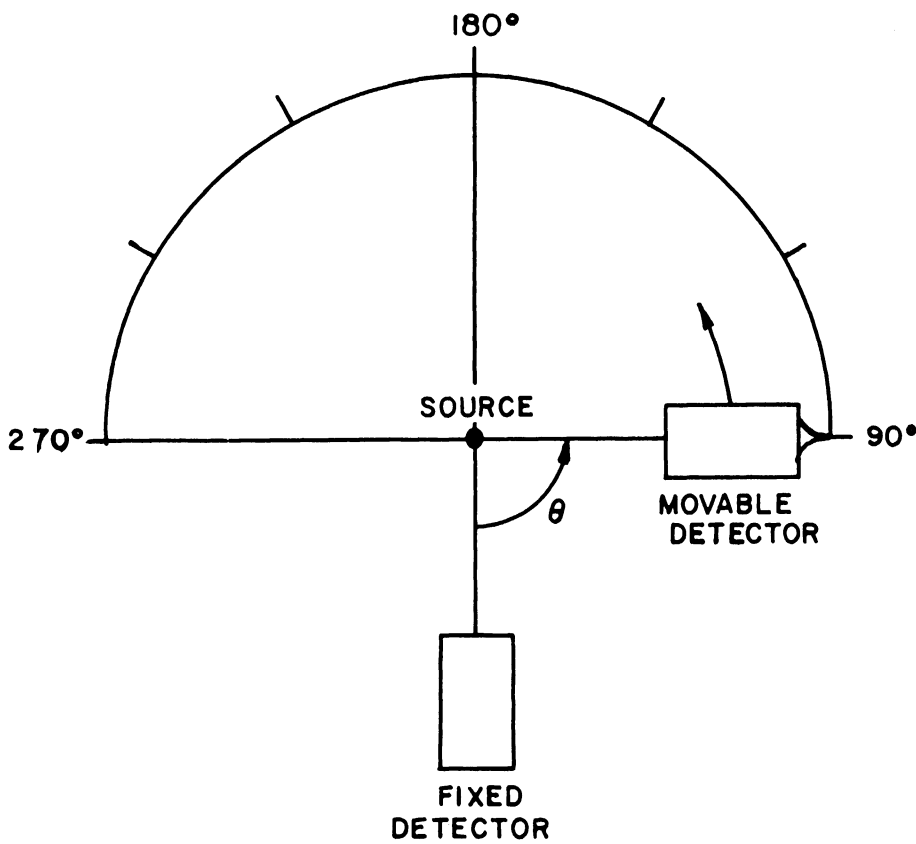
Figure 1. Detector Arrangement

The correlation function is measured experimentally by observing the
number of coincidences per unit time between the two detectors as a func-
tion of the angle Θ between them. Since the correlation function involves
powers of $\cos^2\Theta$, all the information about the correlation can be gained
by taking data in a single quadrant, for example from $\Theta = 90°$ to $180°$.
However, to insure against any possible source misalignment and false
asymmetries due to scattering from nearby objects, data are taken not
only in the quadrant from $90°$ to $180°$ but also in the quadrant from $180°$
to $270°$. The data from the two quadrants are then combined.

Stability

Since a correlation measurement involves a comparison between
coincidence rates at various angles it is extremely important that the
equipment be stable. Because some instability is always present (generally
a steady drift), data should be taken for only a short period of time
at each angle. By running back and forth through the double quadrant
sequence many times the necessary number of coincidences can then be
accumulated, and a steady drift does not cause any difficulty. In addi-
tion, any short term instabilities tend to be averaged out by this
method.

Complex Decay Schemes

If the nucleus being investigated has more than one gamma-
gamma cascade, the interpretation of a single correlation measurement
is complicated by the interference from the other cascades. Since
scintillation counters[36] have energy selective properties the utili-
zation of them as detectors can partially overcome this difficulty.
However, even with energy selection the effect of interference due to
unresolved peaks or Compton background from other gamma rays allows

only a partially effective selection of any one gamma ray. Of course, one important exception to this is the highest energy gamma ray present in the decay.

Accidental Coincidences and Background

In addition to the real coincidences which are due to the simultaneous detection of two gamma rays from the same nucleus there will be accidental coincidences arising from the simultaneous detection of two gamma rays originating in two different nuclei. The term simultaneous is used in the sense that if two counts arrive at the coincidence circuit within the time interval τ, where τ is the resolving time of the coincidence circuit, they will be recorded as being in coincidence. The total coincidence rate N_T is what is actually measured. The real coincidence rate N_R is then given by

$$N_R = N_T - N_A \tag{15}$$

where N_A is the accidental coincidence rate.

For counts occurring in a random time sequence the accidental coincidence rate can be expressed as [37]

$$N_A = 2\tau N_1 N_2 \tag{16}$$

where N_1 and N_2 are the single counting rates. It is desirable that the accidental rate be small compared to the real coincidence rate since an error in the determination of N_A will be reflected as an error in N_R. There are two methods of determining the resolving time using equation (16). One method consists of measuring the coincidence rate from two independent sources while the other method involves using a single source and a delay in one channel much longer than the resolving time τ. In either case, all the coincidences recorded are then accidental coinci-

dences. Knowing N_A and the single rates N_1 and N_2, τ can be calculated from equation (16).

No correction need be made for the background counting rate since energy selection is employed and the single rates are much greater than the background. In addition, any coincidences which are due to the constant background will be corrected for by the process of determining the accidental coincidences.

Resolving Time and Source Strength

In the case of selective counters the real coincidence rate is given by

$$N_R = N\, \sigma_1\, \varepsilon_1\, \sigma_2\, \varepsilon_2 \tag{17}$$

where N is the source strength, σ_1 and σ_2 are the solid angles subtended by the two detectors, and ε_1 and ε_2 are the detection efficiencies for the counters. The single rates are

$$N_1 = N\sigma_1\varepsilon_1 \quad , \qquad N_2 = N\sigma_2\varepsilon_2 \tag{18}$$

Inserting equations (18) into the expression for the accidental coincidence rate, one obtains

$$N_A = 2\tau N^2 \sigma_1\, \varepsilon_1\, \sigma_2\, \varepsilon_2 \tag{19}$$

Dividing equation (19) by equation (17) an expression for the real to accidental ratio is obtained.

$$\frac{N_R}{N_A} = \frac{1}{2\tau N} \tag{20}$$

This ratio should be kept as large as possible in order to reduce the correction to the observed coincidence rate. Since N_R is proportional to N, a lower limit on the source strength N is imposed by the minimum

tolerable real coincidence rate N_R. The maximum value of N is limited in many cases by other factors such as single counting rates. Thus τ , the resolving time, is the prime factor in determining the ratio of real to accidental coincidences, and one would like to make τ as small as possible to give the maximum real to accidental ratio.

A lower limit on τ is imposed by the properties of the scintillator which is used for detection. It can be shown that the re-solving time τ should not be less than the scintillation crystal decay constant τ_d if energy selection is to be maintained and all real co-incidence events are to be registered by the coincidence circuit[38]. The crystal decay constant determines the rise time of the photomultiplier output pulse. For sodium iodide crystals, which are normally used for gamma ray detection because of their good energy resolution, the crystal decay constant is 2.5×10^{-7} sec. This sets a lower limit of approxi-mately 2.5×10^{-7} sec. on the resolving time of the coincidence circuit if the above conditions are to be maintained.

It is possible to obtain a shorter resolving time by utilizing the initial portion of the output pulse to trigger the coincidence circuit. However, this method destroys the energy selection properties of the circuit. The technique of doing this will be described in the following chapter.

In practice, a compromise must be made between the real to accidental ratio and the time needed to obtain the necessary data. The real to accidental ratio should be kept greater than five to one, but if the decay scheme is complex and the branching ratios are low, one must sometimes make it as great as one to one.

Efficiency and Solid Angle Variations

If the source is not centered exactly, the solid angle sub-tended by one detector will vary with the angular position. In addition, the efficiencies $\mathcal{E}_1$ and $\mathcal{E}_2$ for the detection of gamma rays may vary. These effects may produce false asymmetries. A first order correction for these variations is obtained by dividing the real coincidence rate by the two single counting rates N_1 and N_2. Using equations (17) and (18) one obtains

$$N_R' = \frac{N_R}{N_1 N_2} = \frac{N \sigma_1 \mathcal{E}_1 \sigma_2 \mathcal{E}_2}{N^2 \sigma_1 \mathcal{E}_1 \sigma_2 \mathcal{E}_2} = \frac{1}{N} \qquad (21)$$

The corrected real coincidence rate N_R' then depends only on the source strength N and is independent of variations in the solid angles and efficiencies.

Decaying Source

If the half-life of the source is much longer than the time necessary to take the data in one quadrant, no correction need be made for the source decay. For a short half-life source, taking the data in the order $90° \rightarrow (90° + \theta) \rightarrow (270° - \theta) \rightarrow 270°$ provides a first order correction for the decay. The data from $90°$ and $270°$ are added together, the data from $120°$ and $150°$ are added together, etc.

Effect of Finite Solid Angle and Source Extension

Since each detector subtends a finite solid angle, the two detectors do not define a single angle θ but instead a range of angles from θ_1 to θ_2. (Figure 2) It has been shown by Frankel[39] that this effect merely attenuates the correlation.
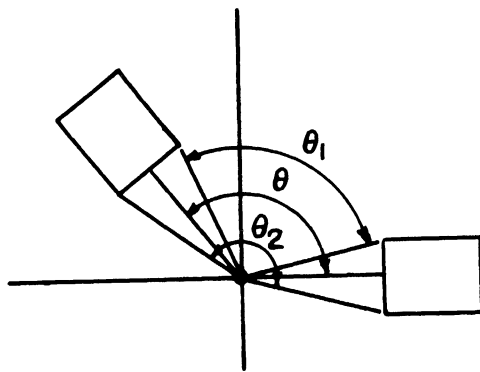
Figure 2. Finite Solid Angle Subtended by Detectors

The measured correlation function can be written (39-42)

$$W'(\theta) = \sum_{\substack{k=0 \\ (k \, even)}}^{k_{max}} G_k A_k P_k (\cos \theta) \qquad (22)$$

where A_k are the expansion coefficients which depend only on the param-
eters of the cascade and G_k are the attenuation coefficients. The G_k

are functions of the efficiency of the detectors, the dimensions of the

scintillation crystal, and the distance from source to crystal. The

efficiency is a function of the gamma ray energies and the angle between

the counter axis and the propagation direction of the gamma rays.

Several methods can be used to determine G_k.

1. The most accurate method of determining the G_k is to

measure the angular efficiencies of each detector for each

energy by means of a collimated beam of gamma rays. The G_k

can then be found by a numerical integration[42,43].

2. If the energies are not too different from 511 kev,

annihilation radiation can be used to determine the counter

resolution. The attenuation coefficients are then found by

a numerical integration over the resolution curve. The expressions for G_k have been tabulated up to G_4 for the case where the resolution curve can be approximated by a triangular or Gaussian distribution.[40]

3. The G_k can be calculated for a given geometry as a function of the absorption coefficient μ of the crystal. Rose[41] has tabulated the attenuation coefficients G_2 and G_4 for 1-1/2" by 1" cylindrical NaI crystals for source distances of 7 and 10 cm. and for values of μ from 0.12 cm^{-1} to 40 cm^{-1}.

For the geometry used in this experiment, namely 2" by 2" NaI (Tl) crystals at a distance of 10 cm. from the source, it was found that methods 1 and 2 yield results for G_k which are equal within experimental error for gamma energies between 500 kev and 2 Mev[43].

The only correction for source size that has been rigorously treated is that for an axially extended cylindrical source[43,44]. It was found that for the above geometry the correction for axial extension was negligible for sources less than 1 cm. in length.

<u>Extranuclear Field Effects</u>

It was mentioned in Chapter I that the correlation function can be attenuated by extranuclear fields. However, if a source is in the form of a dilute solution, the theoretical correlation can be completely restored, or if the interaction is very large, it can be partially restored[30,31]. This is due to the fact that in a liquid there are continual rearrangements of the perturbing fields because of molecular collisions. The extranuclear field may be reoriented many times during

the lifetime of the intermediate state, and the net effect will not cause the nucleus to undergo a large precession. Usually the intermediate state lifetimes are short enough so that the effects of extranuclear fields are not serious.

Scattering Effects

Another problem which must be considered in angular correlation is scattering. Effects due to scattering can mask the true correlation. The scattering of gamma radiation in the source, the scattering from one crystal to the other, and the scattering of radiation from nearby objects can all produce false asymmetries in the measured correlation.

The correction for scattering in the source is complicated and difficult to apply[21]. However, it is usually negligible for high energy gamma rays (greater than 500 kev) and for sources with low atomic number Z. The source should be made as narrow as possible and contained in a holder constructed of a material with a low Z and with as thin a wall as possible to minimize scattering effects. In addition, the use of energy selection helps to reduce the effect of scattering in the source.

Crystal to crystal scattering can cause false asymmetries since a photon can enter one crystal and be partially absorbed and partially scattered. The scattered photon can then enter the other detector and be absorbed, with this event being registered as a coincidence[45]. One method of avoiding coincidences due to this effect is to shield the crystals with lead. Then a scattered photon must traverse two thicknesses of lead while the primary photon must only pass through a single thickness. A second method makes use of energy selection, with the scattered photon not being counted since it necessarily has a lower energy than

the primary photon. In some cases both methods must be used simultane-
ously. The effect of scattering from nearby objects is likewise com-
batted by the use of lead shielding and energy selection.

CHAPTER III

EXPERIMENTAL PROCEDURE

Apparatus

General Description

In Chapter II it was pointed out that a coincidence circuit with both a short resolving time and pulse height selection is needed to investigate directional correlations of cascades occurring in nuclei with complex decay schemes. The so-called method of parallel channels provides a means for achieving this. Two parallel channels are utilized, one of which provides the short resolving time and the other, the energy selective properties. A coincidence circuit employing this method is called a fast-slow coincidence spectrometer. The reason for this nomenclature will be seen later.

A block diagram of the fast-slow coincidence spectrometer used in this experiment is shown in Figure 3. The apparatus was designed and built by R. Scharenberg and M. Stewart[46,47]. Scintillation counters were used as gamma ray detectors, and each counter fed both a fast and a slow channel which were in parallel. The fast channels led to a fast coincidence circuit with a resolving time of about 8×10^{-9} sec. The fast coincidence circuit recorded a count when any pair of gamma rays were in coincidence. The output of this was fed into a slow triple coincidence circuit ($\tau \sim 2 \times 10^{-7}$ sec.) along with the energy selected pulses from the slow channels. If the discriminator in slow channel 1 selects only a single gamma energy γ_i and the discriminator in slow channel 2 selects only γ_j, then the gate circuit (triple coincidence circuit) will give a count only when the fast coincidence is between
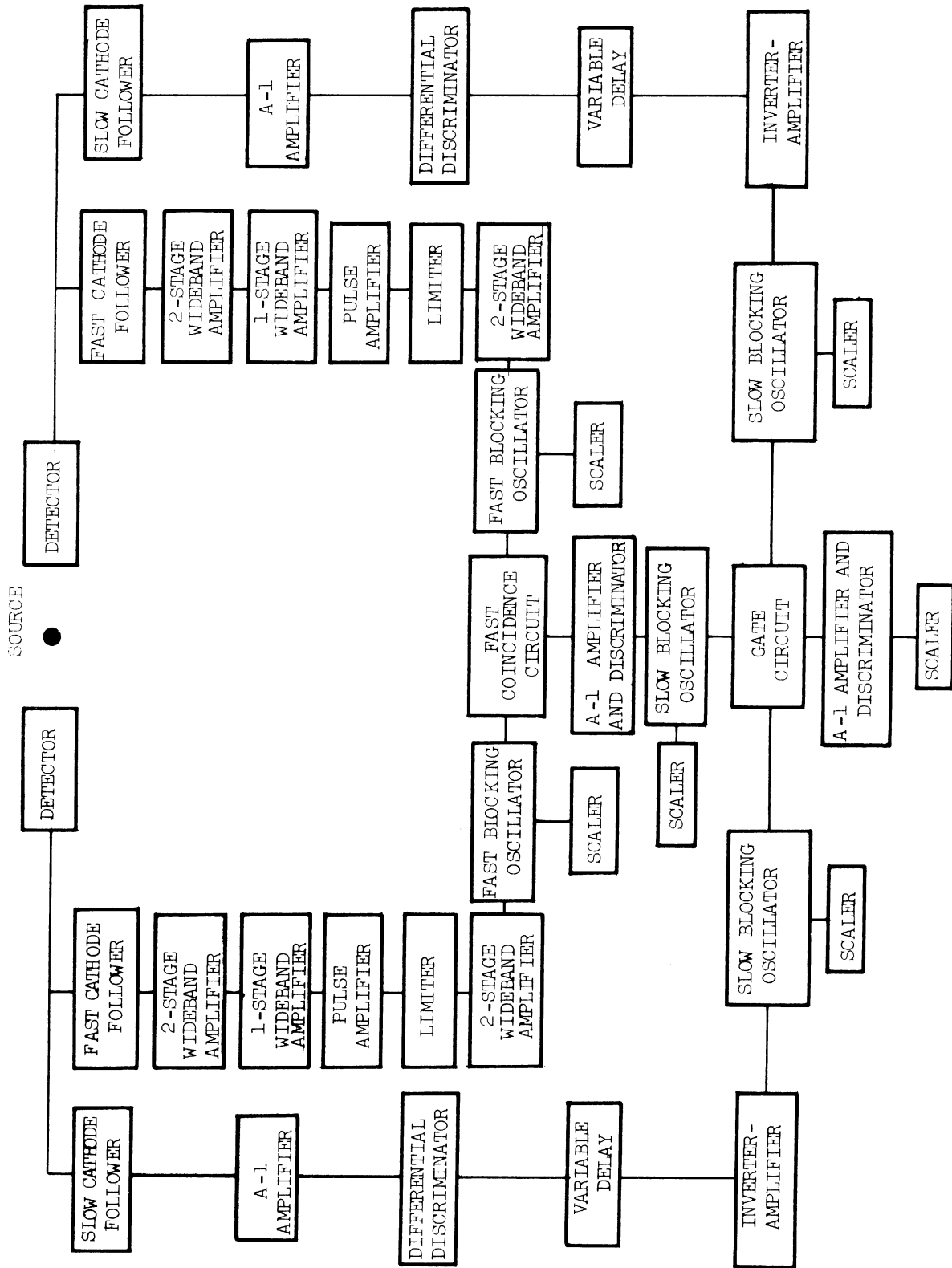
Figure 3. Block Diagram of Apparatus

γ_i and γ_j. The effective resolving time of this fast-slow coincidence circuit is determined principally by the fast coincidence circuit resolving time and is approximately 1×10^{-8} sec.

Since the details of the electronic circuits have been thoroughly described by Scharenberg and Stewart[46,47], only a brief description of the apparatus will be presented here.

Source Mounting

The sources used in this experiment were liquids. The source material was contained in a cylindrical cavity 1/8" in diameter and 3/8" in length drilled in a lucite holder (Figure 4). The wall was approximately 1/32" thick. The source holder was held at a height of about 5" above the table by a brass rod, and in all correlation measurements the source to crystal distance was 10 cm.

LUCITE CAP
SOURCE
LUCITE HOLDER
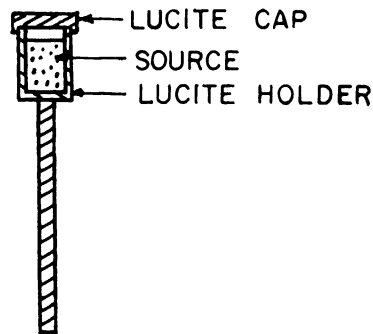
Figure 4. Cross-Section of Source Holder

Detectors

The gamma ray detectors consisted of commercial NaI (Tl) crystals mounted on RCA 6342 photomultiplier tubes. The crystals were cylindrical in shape, 2" in diameter and 2" thick, and were coupled to the end of the phototubes using Dow-Corning 200 Silicone oil (viscosity $= 10^6$ poise). The phototubes were magnetically shielded with mu-metal

shields. Each phototube was mounted inside a 2-1/2" iron pipe with the crystal projecting through the front cap.

Aluminum shields 3/16" thick were placed between the crystals and the source to stop beta particles from entering the crystals. Lateral lead shielding was used in some of the correlation measurements to prevent counter to counter scattering when it could not be eliminated by energy selection.

Fast Channels

Since the resolving time of a coincidence circuit is of the order of the width of the input pulses it is necessary to produce pulses of about 10 millimicroseconds duration if a resolving time of 1×10^{-8} sec. is desired, and if each pulse is to produce the same effect on the coincidence circuit, they should be uniform in shape and size. In addition, the pulses should have a fast rise if no jitter is to occur in firing the coincidence circuit (due to the fact that scintillation counter pulses with different amplitudes are delayed by different amounts). Thus the slow-rising, long-duration, non-uniform pulses from the scintillation counter must be converted to uniform pulses with a fast rise and short duration. This is accomplished at the expense of losing all information about the amplitude of the pulse (and therefore the energy of the incident radiation).

The negative output pulse (0.5-5 v.) from the scintillation counter is fed first into a fast cathode follower which has a gain of about about 0.5. From here the pulse is sent through 200 ohm coaxial cable into a series of three 100 megacycle transmission line amplifiers (Hewlett-Packard types 460A and 460B) each of which has a maximum gain

of about eight. Fast amplifiers must be used since the high frequency
components of the pulse must be amplified to produce a fast rising pulse.

The first amplifier is a two-stage linear amplifier, and the
second is a single-stage linear amplifier. Both of these saturate at
about eight volts into a 200 ohm load. The third amplifier is a pulse
amplifier which saturates at about sixty volts. The pulse amplifier will
amplify only a positive signal. With the maximum gain available, all
pulses corresponding to gamma ray energies of about 200 kev or higher
saturate by the time they reach the pulse amplifier. The pulse amplifier
adds no further saturation and produces a negative output pulse of about
60 volts. This large negative pulse is then fed into a limiter circuit
consisting of a sharp cut-off pentode which cuts off with a one-volt
signal on the grid. This produces a very fast rising pulse (5×10^{-9}
sec.). Since the plate resistor in the limiter must be small to obtain
a fast rise the gain of the limiter is small. Another two-stage wideband
amplifier is used to amplify the small limiter pulse. As soon as satura-
tion occurs in the fast amplifiers, all information about the original
pulse height and gamma ray energy is lost.

The amplified limiter pulse (15 v. positive) is fed into a
fast blocking oscillator circuit[48] employing subminiature components.
The blocking oscillator produces a uniform positive pulse of about 40 v.
with a 10^{-8} sec. rise and 6×10^{-8} sec. duration.

Since a negative pulse is needed for the coincidence circuit
an inverting stage is used to convert the positive blocking oscillator
pulse to a negative pulse. The inverter tube saturates very quickly pre-
serving the fast rise and gives a 7 v. flat-topped negative pulse. A

shorted delay line is then used to clip the pulse width to 2×10^{-8} sec.
The final pulse is 7 v. negative with a rise time of about 1×10^{-8} sec.
and a duration of about 2×10^{-8} sec.

The pulses from the two fast channels are fed into a Garwin type coincidence circuit[49,50]. The Garwin coincidence circuit is used because of its fast resolving time and good discrimination ratio of coincidence pulses to singles pulses. The output of the fast coincidence circuit is sent to an amplifier and discriminator (Atomic model 204B) which passes the coincidence pulses but not the singles pulses.

Since the electrical lengths of the two fast channels are dependent on the amplifier gain settings, blocking oscillator bias voltage, etc., the channel lengths must be aligned properly. This is accomplished by adjusting the coaxial cable lengths.

Slow Channels

The function of the slow channels is to amplify the scintillation counter pulses and select pulses which have amplitudes between some predetermined limits. As mentioned previously, the energy selection channels (slow channels) are placed in parallel with the fast channels. The pulse from the scintillation counter is fed first into a slow cathode follower which has a gain of about 0.25, and from there into an A-1 amplifier (Atomic model 204B). The output of the A-1 amplifier is fed into a differential discriminator circuit which was designed by Lu[51]. The discriminator output is sent through a variable delay and single-stage amplifier into the slow blocking oscillator circuit. The variable delays provide an adjustment to align the slow channels. The slow blocking oscillators are almost identical to the fast blocking oscillators, the

main difference being the use of a pulse transformer that gives a 0.2 microsecond pulse width rather than the 0.06 microsecond width as in the fast channels. The outputs from the two energy channels together with the fast coincidence output are then put in triple coincidence. The gate circuit (triple coincidence circuit) is a Garwin type circuit, and the resolving time (2×10^{-7} sec.) is determined by the 0.2 microsecond width input pulses. The output of the gate circuit is sent to an amplifier and discriminator where the smaller singles and doubles pulses are rejected and the triple coincidence pulses are passed on to a scaler.

Scalers

Six scalers are connected so as to record the fast singles counting rates, the slow singles counting rates, the fast coincidence rate, and the gate coincidence rate. The scalers are the conventional binary type scalers. The fast singles rates and the fast coincidence rate are merely used as a check on the performance of the fast channels while the slow singles rates are used to correct the observed gate coincidence rate for solid angle variations, efficiency variations, and source decay.

Stability

It was mentioned in Chapter II that stability is very important if accurate correlation measurements are to be made. The problem of stability is reduced if the power and voltage sources are regulated properly.

The 110 v. A.C. power was regulated to $\pm$ 0.1% by means of Sorensen regulators, except for the scaler power which was not critical. The separate D.C. voltage supplies were also regulated to about $\pm$ 0.2%,

with special care being exercised with the phototube supply which was regulated to within $\pm$ 0.01%. The equipment was operated in an air-conditioned room which made all temperature effects negligible. With the precautions taken, the energy selected counting rates were stable to within $\pm$ 2% and all other counting rates to within $\pm$ 1%.

Procedure in A Typical Correlation Measurement

The procedure followed in making the angular correlation measurement was approximately the same for all the correlations which were run.

Alignment of Apparatus

First, the source was centered properly so that the solid angle remained constant as the movable detector was rotated from 90° to 270°.

Second, the fast and slow channels were aligned. Since different energies and counting rates could affect the electrical lengths, the same source and discriminator settings which were to be used in the correlation measurement were also used in the alignment. The gain of the fast amplifiers was adjusted so that the lowest energy of interest saturated the limiter. The alignment of the fast channels was accomplished by observing the fast coincidence rate as a function of the relative cable length in the two channels. Since the resolving time is about ten millimicroseconds and the delay in the cable is one millimicrosecond per foot, the alignment process can be done with a relatively small amount of cable. The energy channels would require several hundred feet of cable to align by this method, so they were aligned with the aid of a Tektronix 517 oscilloscope. Delay cable was added after the fast coincidence output until the fast coincidence pulses arrived at the gate circuit last. These

pulses were used to trigger the oscilloscope, and the slow channel singles pulses were applied to the vertical input. The variable delays in the slow channels were adjusted until the singles pulses appeared at the beginning of the sweep.

Correlation Measurement

The data was normally taken at 15° intervals in the double quadrant sequence, running for 5 minutes at each angle. This procedure was continued until sufficient statistics were obtained. The total number of coincidences accumulated depended on the magnitude of the correlation asymmetry, the real to accidental ratio, and the coincidence counting rate. If the counting rate is very low, one must settle for poorer statistics since it is not advisable to run the correlation over too long a period of time because of stability problems.

The accidental coincidence rate was measured by the double source method after every three or four sweeps through the double quadrant sequence. The counting rates and discriminator settings which were used in the accidental measurement were the same as those used in the actual correlation measurement. This allowed an accurate determination of the accidental rate. For the Cd^{110} measurements, the real to accidental ratio was always greater than ten to one, while for Se^{76} the ratio was always greater than five to one.

Data Analysis

After correcting for the accidental counting rate, the coincidence rate was normalized by dividing by the two energy channel singles rates N_1 and N_2. In the case of Se^{76}, the coincidence rate was divided by N_1 and N_2 and multiplied by $N_1(180°) \cdot N_2(180°)$. The reason for this was that the division by $N_1 N_2$ makes the normalized coincidence

rates at the end of the measurement much larger than those at the begin-ning of the measurement because of the source decay. In the process of making a weighted least-squares fit to the data this gives a false statis-tical weight to the later measurements. By multiplying by $N_1(180°)$ $N_2(180°)$ this difficulty is overcome. The method of taking data in the double quadrant sequence provided sufficient correction for the source decay here.

After all the data for a given angle were added together, a least-squares fit of the data was made to the function

$$W(\theta) = 1 + A_2' P_2(\cos\theta) + A_4' P_4(\cos\theta)$$

The procedure in making the least-squares fit has been extensively treated by Rose[52]. The annihilation radiation from Na^{22} was used to correct for the effect of finite angular resolution. This correction was applied to the normalized expansion coefficients A_2' and A_4' giving the corrected coefficients A_2 and A_4. After the corrected coefficients A_2 and A_4 were obtained, they were compared with the theoretical results for all possible values of the cascade parameters.

CHAPTER IV

RESULTS OF GAMMA-GAMMA DIRECTIONAL
CORRELATION MEASUREMENTS IN Se^{76}

Introduction

As^{76} decays by complex beta emission to Se^{76} with a half-life

of 26.8 hours. The decay scheme of As^{76} has been the subject of many

investigations[53-57]. The presently accepted scheme was first proposed

by Kraushaar and Goldhaber[56] and later confirmed by Kurbatov, Murray,

and Sakai[57]. The decay scheme presented by Kurbatov, et al.[57], is

shown in Figure 5. The numbers in parentheses are the relative gamma

intensities. The log ft values for the beta transitions and their in-

terpretation are given in Table 1.

TABLE 1. As^{76} BETA DECAY DATA

Beta Energy (Mev)	Log ft	Interpretation
2.97	8.8	Unique 1st Forbidden ($\Delta J = 2$, yes)
2.41	8.2	1st Forbidden ($\Delta J = 0, \pm 1$; yes)
1.76	7.9	1st Forbidden ($\Delta J = 0, \pm 1$; yes)
0.36	6.1	1st Forbidden ($\Delta J = 0, \pm 1$; yes) or Allowed ($\Delta J = 0, \pm 1$;, no)

The ground state spin of As^{76} has been measured to be 2 by an

atomic beam method[58]. This agrees with the value of 2$^-$ predicted by

Nordheim's rules[59].

-33-
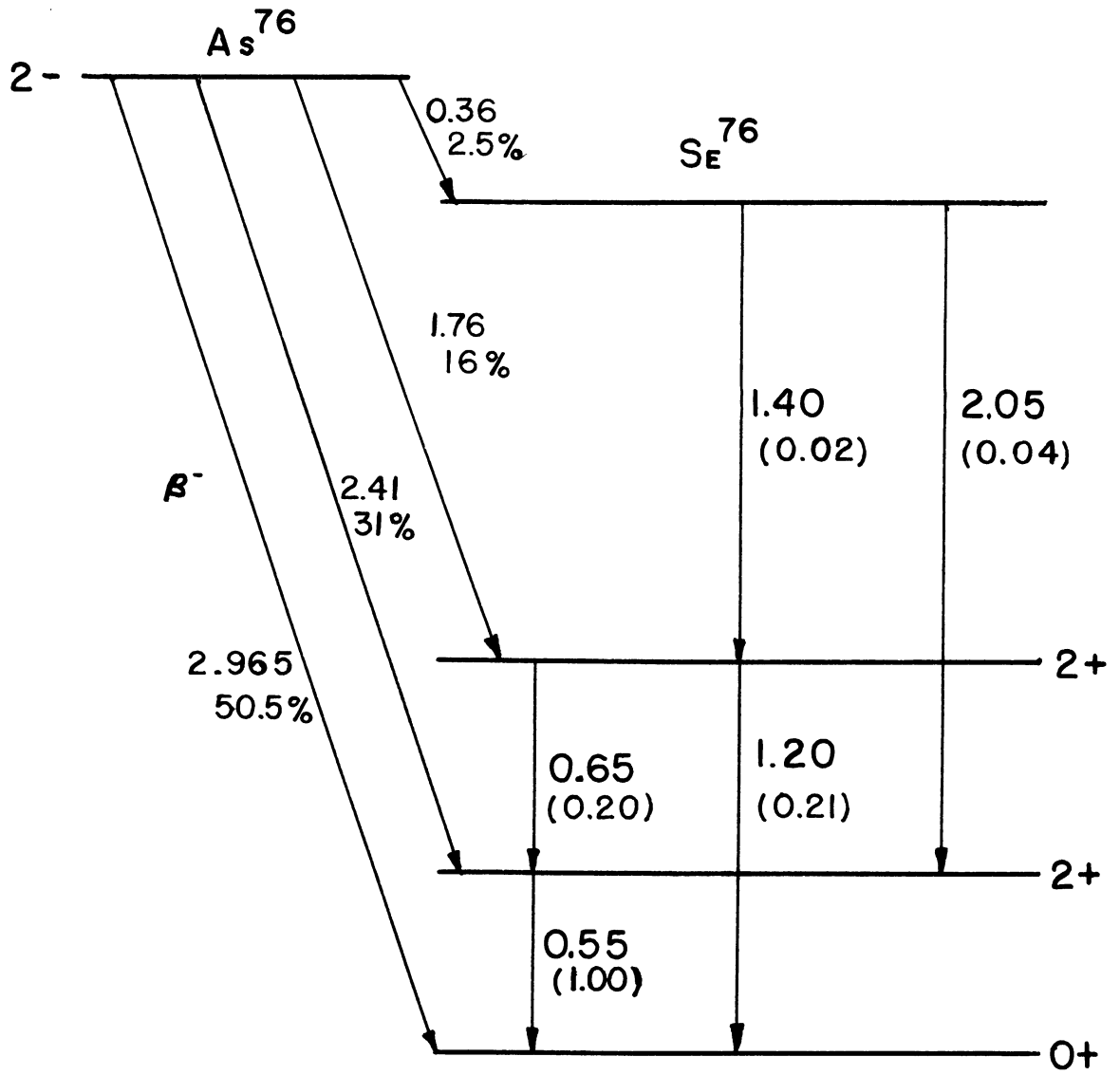
Figure 5. Decay Scheme of As^{76}

Directional correlation measurements have been made previously on the 0.65 Mev - 0.55 Mev and 1.40 Mev - 1.20 Mev cascades. Kraushaar and Goldhaber[56] measured the 0.65 - 0.55 correlation without using energy selection and assigned spin 2^+ to both the 0.55 Mev and 1.20 Mev levels (assuming a 0^+ ground state) with the 0.65 Mev gamma ray consisting of 34 to 80 percent E2 radiation and the remainder M1 radiation. Metzger and Todd[60] repeated this correlation using pulse height selection and confirmed the 0^+ - 2^+ - 2^+ assignment. Their results indicated that the 0.65 Mev gamma ray is almost pure electric quadrupole radiation ($Q > 85\%$).

Wiedling[61] recently reported a measurement of the 1.40 Mev - 1.20 Mev directional correlation. The results agreed very well with a 3(D)2(Q)0 sequence. Wiedling made an assignment of 3^- to the 2.60 Mev level with the 1.40 Mev gamma transition being pure E1 radiation. This assignment of negative parity to the 2.60 Mev level was made on the basis of relative gamma intensities, the log ft value for the 0.36 Mev beta transition, and the fact that the lowest odd spin state in an even-even nucleus usually has odd parity. However, none of these allow a unique determination of the parity of the 2.60 Mev level.

Kurbatov's log ft values (Table 1) are in good agreement with the assignment of 0^+, 2^+, 2^+ to the three lowest levels in Se^{76}, but the value of 6.1 for the 0.36 Mev beta lies on the borderline between an allowed and first forbidden transition. No definite assignment can be made to the 2.60 Mev level from this log ft value although Kurbatov preferred 3^+.

In the present investigation, correlation measurements were

made on the 2.05 Mev - 0.55 Mev cascade for the first time. In addition,
the 1.40 Mev - 1.20 Mev and 0.65 Mev - 0.55 Mev directional correlations
were remeasured to provide a check on the previous investigations and to
see whether a more accurate result could be obtained for the mixture in
the 0.65 Mev transition.

The source material was obtained from Oak Ridge. It was in
the form of arsenic dissolved in dilute hydrochloric acid. Small amounts
of Sb^{122} and Sb^{124} were present in the source material. The decay was
carefully studied, and it was found that the effect of the contamination
on the correlations was negligible. The observed gamma ray spectrum,
Figure 6, was in agreement with the decay scheme reported by Kurbatov,
et al.[57]

The mean lifetime of the first excited state has been measured
to be $(3.3 \pm 2.2) \times 10^{-11}$ sec.[62], and the lifetime of the 1.20 Mev
state is expected to be short. Because of this and the fact that the
source was in a dilute solution the measured correlation functions should
not be attenuated due to extranuclear field effects.

For each correlation the discriminators were set in such a way
that there was no interference from any of the other cascades. Thus the
full correlation was measured in each case.

Results and Interpretation

0.65 Mev - 0.55 Mev Correlation

Both differential discriminators were set at position A as
shown in Figure 6 so as to include both the 550 kev and 650 kev photo-
peaks. Lateral lead shielding was used for this correlation. The data
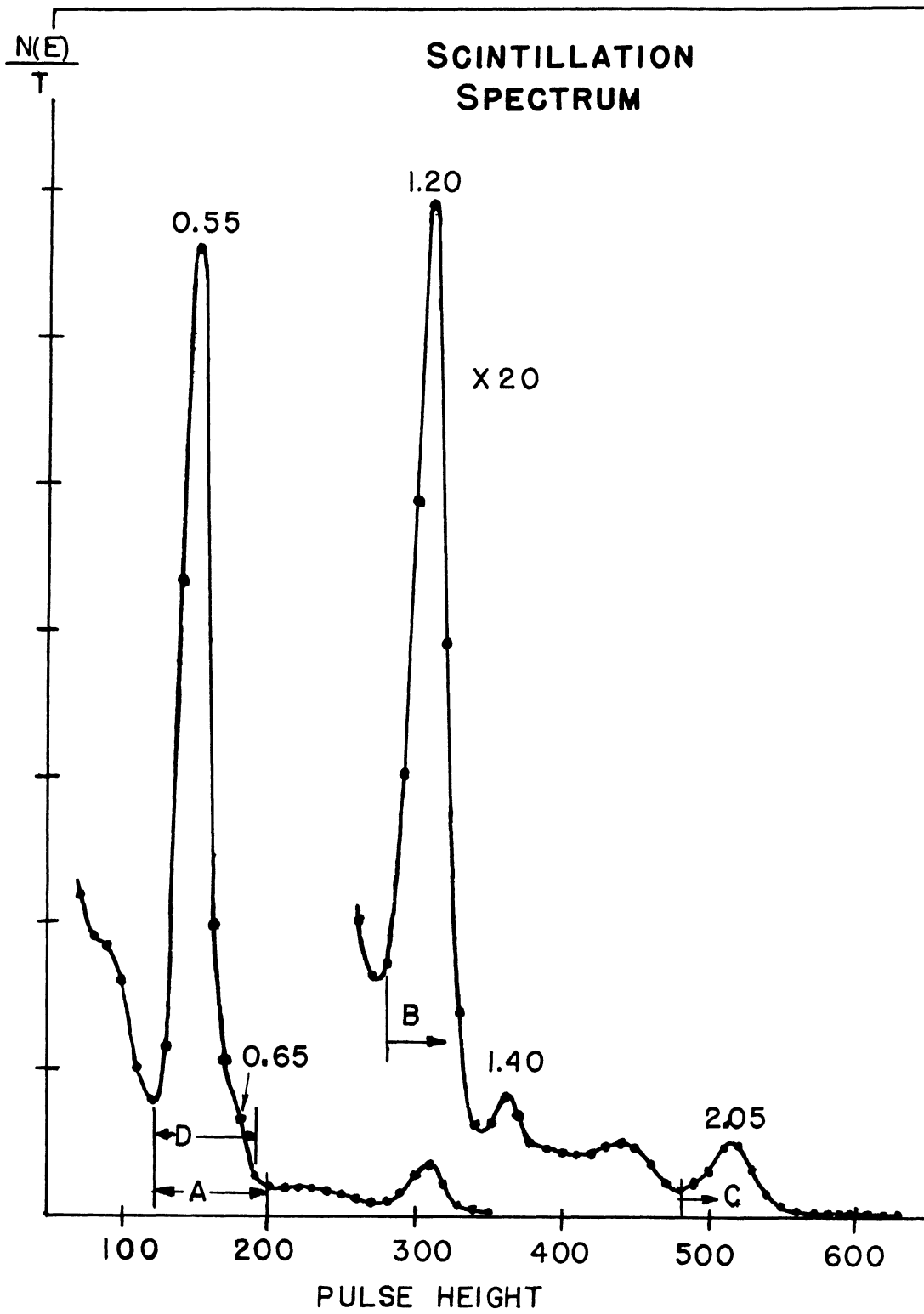
Figure 6. Se[76] Gamma Ray Spectrum

are shown in Figure 7. The solid curve is the least squares curve corrected for finite geometry, and the error flags indicate the root-mean-square statistical errors of the experimental points. The broken curve is a plot of the theoretical correlation function for a pure $2(Q)2(Q)0$ cascade. The experimental values of the expansion coefficients corrected for finite geometry are $A_2 = -0.042 \pm 0.015$ and $A_4 = 0.319 \pm 0.023$. The errors quoted are those defined by Rose in Equation 30 of reference (52). If one assumes a spin of 0^+ for the ground state of Se^{76} (even-even nucleus), the experimental coefficients are not compatible with any combination of spins considering pure dipole or quadrupole radiation. If a mixture in the 650 kev transition is considered, only the $2(D,Q)2(Q)0$ sequence will fit the data. In Figure 8 the values of A_2 and A_4 are plotted vs. Q, the quadrupole content, for a $2(D,Q)2(Q)0$ sequence. The error flags represent the experimental values of A_2 and A_4. From Figure 8 it is seen that the data are consistent with a value of Q equal to 0.997 ± 0.002.

It can thus be concluded that the first and second excited states have spins of 2^+ and that the 650 kev gamma transition is a mixture of $(99.7 \pm 0.2)\%$ electric quadrupole and $(0.3 \pm 0.2)\%$ magnetic dipole radiation. This result is in agreement with the value of $Q > 0.85$ found by Metzger and Todd[60]. However, the results of the present investigation restrict the quadrupole content of the 0.65 Mev transition to much smaller limits than found in the previous measurements. Subsequent to the present investigation, Lindqvist[63] reported another measurement of the 0.65-0.55 correlation. He found a value of $Q = 0.98 \pm 0.01$. However, Lindqvist's data was taken at only three angles.

Figure 7.   0.65 Mev - 0.55 Mev Directional Correlation in Se[76]
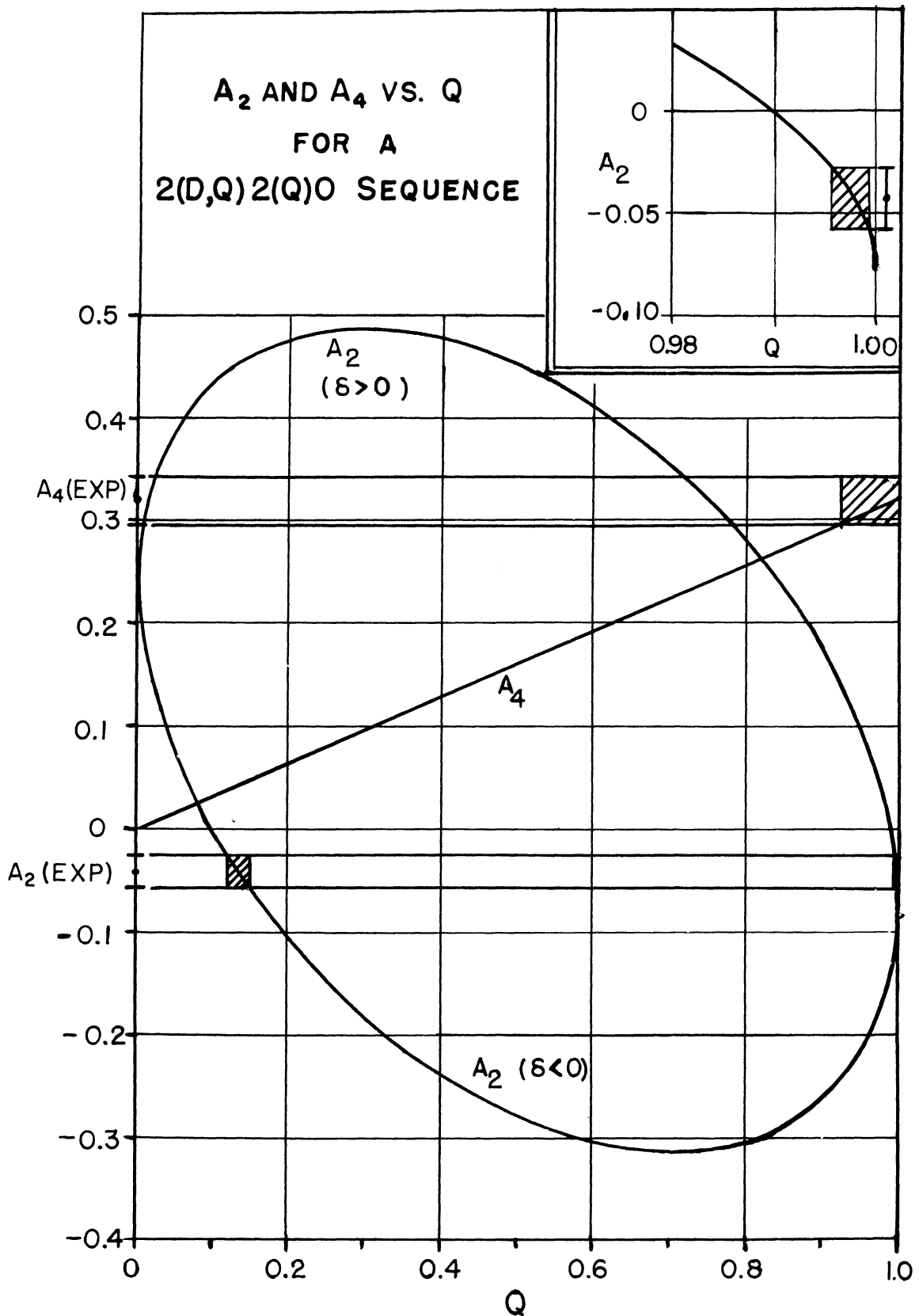
Figure 8. A_2 and A_4 vs. Q for a 2(D,Q)2(Q)0 Sequence

2.05 Mev - 0.55 Mev Correlation

For the 2.05 Mev - 0.55 Mev correlation one discriminator was set integrally at C and the other differentially at D as shown in Figure 6. Lateral lead shielding was used for this correlation. Because of the low coincidence rate, data were taken at only four angles. The experimental data and least squares curve corrected for finite geometry are shown in Figure 9. The corrected coefficients are A_2 = -0.027 $\pm$ 0.022 and A_4 = -0.075 $\pm$ 0.033. The negative value for A_4 rules out the combinations $4(Q)2(Q)0$ and $2(D,Q)2(Q)0$ since both require a positive A_4. The data can best be explained by the sequence $3(D,Q)2(Q)0$. In Figure 10 the theoretical values of A_2 and A_4 are plotted vs. Q, the quadrupole content of the 3-2 transition. It is seen that the experimental values of A_2 and A_4 are compatible with a value of Q = 0.948 $\pm$ 0.014. Since an E1-M2 mixture of this magnitude is very unlikely it is reasonable to conclude that the 2.05 Mev gamma ray consists of (94.8 $\pm$ 1.4)% E2 and (5.2 $\mp$ 1.4)% M1 radiation. On the basis of this and the selection rules for gamma transitions, a value of 3^+ can be assigned to the 2.60 Mev level. This assignment agrees with that of Kurbatov, et al.[57], which was made on the basis of log ft values and relative intensities, but the + parity disagrees with Wiedling's assignment[61].

The data can almost be explained by a $1(D,Q)2(Q)0$ sequence. However, a spin of 1 for the upper level is very unlikely because of the absence of the 2.60 Mev crossover transition.

1.40 Mev - 1.20 Mev Correlation

For this correlation the discriminators were both set integrally at position B (Figure 6) so as to include everything above the 1.20 Mev
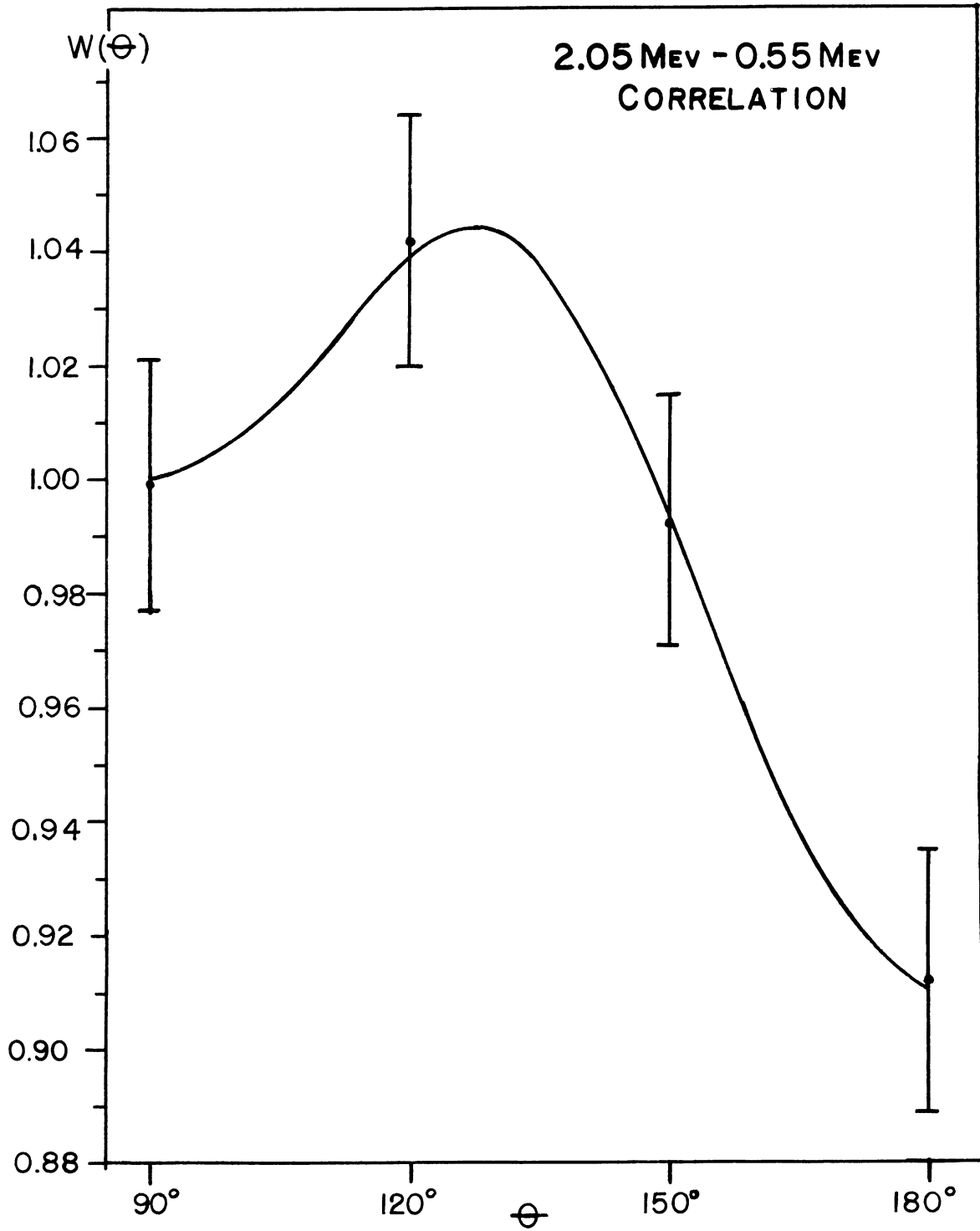
Figure 9. 2.05 Mev - 0.55 Mev Directional Correlation in Se[76]

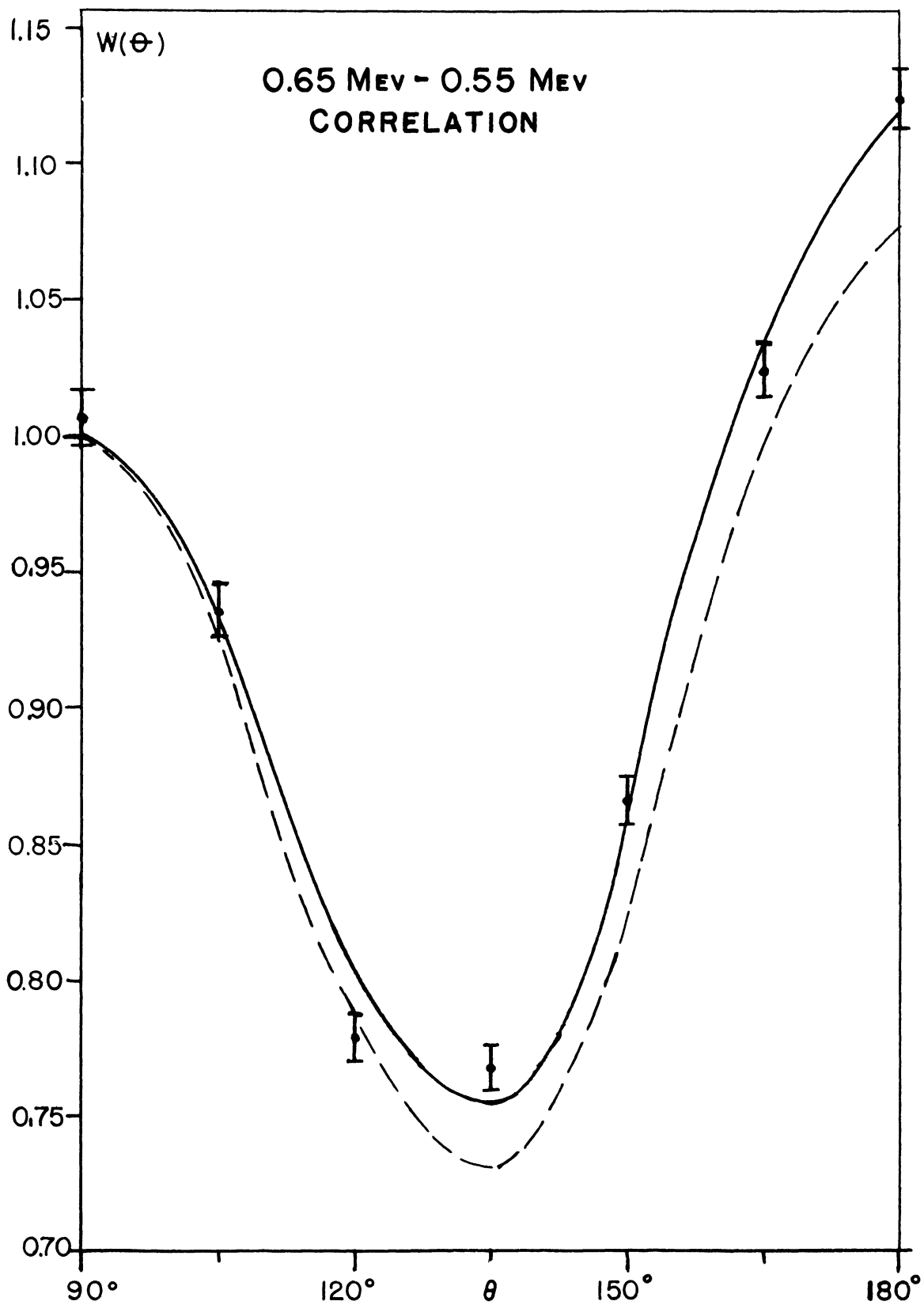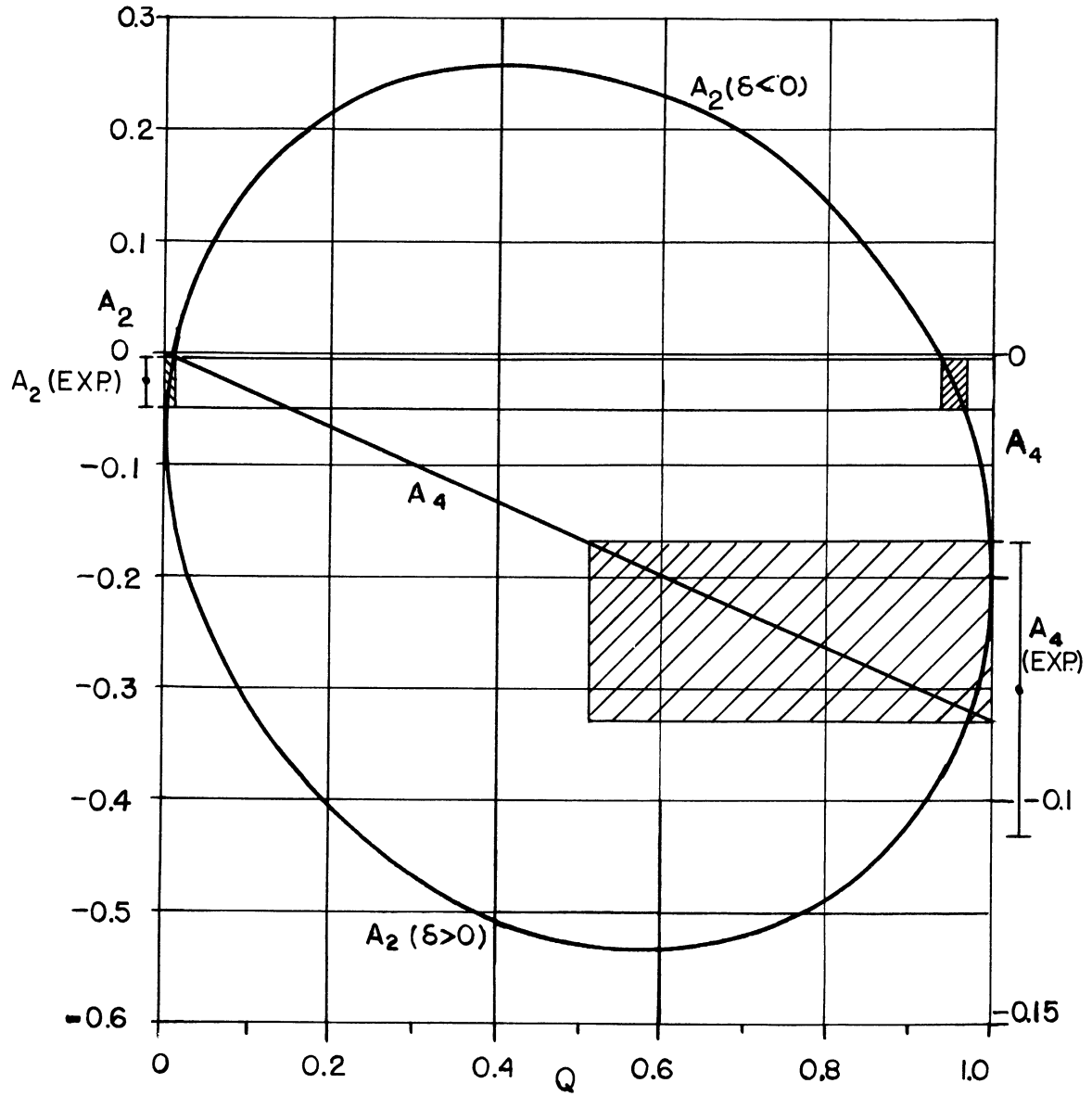Figure 10. A_2 and A_4 vs. Q for a $3(D,Q)2(Q)0$ Sequence

photopeak. No lateral lead shielding was needed. The data are shown

in Figure 11, the solid curve being the least squares curve corrected

for finite geometry and the dotted curve the theoretical curve for a

$3(D)2(Q)0$ combination. The corrected experimental coefficients are $A_2 =$

-0.076 ± 0.022 and $A_4 = -0.003 \pm 0.032$. It is seen that the error in

A_4 is ten times larger than the coefficient itself. Thus the existence

of any A_4 is questionable. When only A_2 is considered, a value of $A_2 =$

-0.077 ± 0.019 is obtained. This is in good agreement with the theoreti-

cal value of $A_2 = -0.0714$ for a $3(D)2(Q)0$ cascade. Considering this se-

quence, the maximum amount of quadrupole admixture in the 3-2 transition

consistent with the data is 0.05%. The data can also be explained by

the sequence $1(D,Q)2(Q)0$. However, the possibility of spin 1 for the

2.60 level has already been ruled out.

Therefore the results of the 1.40 - 1.20 correlation confirm

the spin assignment of 3 to the 2.60 Mev level in Se^{76}. Since a positive

parity for this state is necessary to explain the 2.05 - 0.55 correlation

it is concluded that the 1.40 Mev gamma ray must be M1 radiation. Wiedling

had assigned E1 radiation to the 1.40 Mev transition assuming a negative

parity for the 2.60 level.

Summary and Discussion

The results of the correlations confirm the assignment of 0^+,

2^+, 2^+, 3^+ to the energy levels of Se^{76} in order of increasing energy.

The 0.55 Mev and 1.20 Mev gamma rays are found to be pure E2 radiation,

the 0.65 Mev gamma ray $(99.7 \pm 0.2)\%$ E2 and $(0.3 \mp 0.2)\%$ M1, the 2.05 Mev

gamma ray $(94.8 \pm 1.4)\%$ E2 and $(5.2 \mp 1.4)\%$ M1, and the 1.40 Mev gamma

ray almost pure M1 $(<0.05\%$ E2).
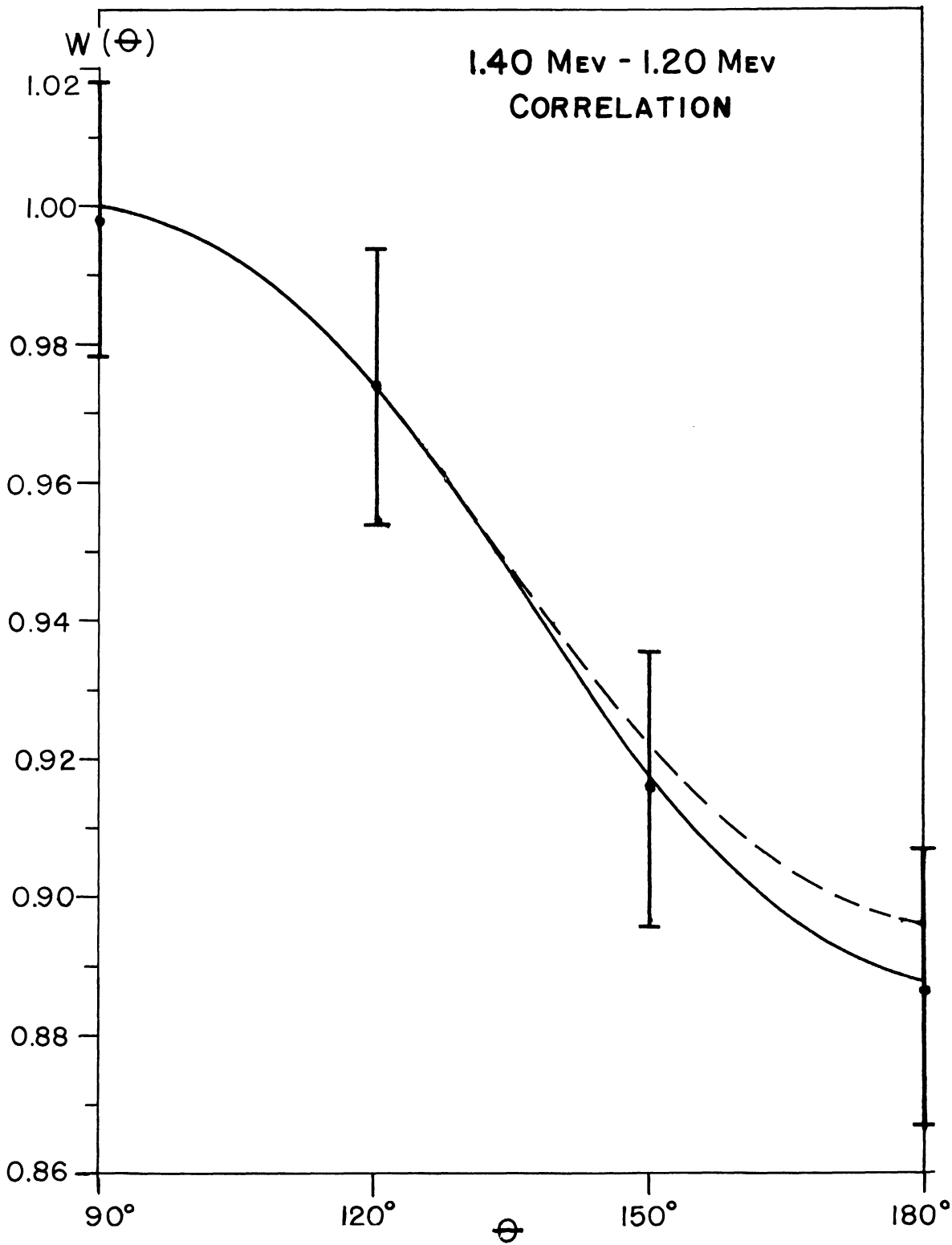
Figure 11.   1.40 Mev - 1.20 Mev Directional Correlation in Se[76]

These results are difficult to explain in terms of an individual particle model. If one calculates the ratio of E2 to M1 transition probabilities using Rose's theoretical estimate for the transition of a single proton[64], the following results are obtained for the gamma transitions in Se^{76}.

$$\left[\frac{I(E2)}{I(M1)}\right]_{2.05\,MEV} = 0.08$$

$$\left[\frac{I(E2)}{I(M1)}\right]_{1.40\,MEV} \simeq 0.04$$

$$\left[\frac{I(E2)}{I(M1)}\right]_{0.65\,MEV} = 0.009$$

Therefore appreciable E2 admixtures are not expected in any of these gamma rays according to a strict individual particle model.

Almost all even-even nuclei have a spin of 2^+ for the first excited state, and in many cases the second excited state is also 2^+. Table 2 lists several of these nuclei[65]. The energies of the first and second excited states, E_2 and E_2', are given in columns two and three and their ratio E_2'/E_2 in column four. There are some noticeable regularities here. As one goes farther from the closed shell values N = 28, 50, 82, and 126, the E_2 and E_2' values become smaller. However, the ratio E_2'/E_2 is approximately constant for all cases listed, having a mean value of about 2.2.

The fifth column gives the E2 transition probability from the ground state to the first excited state in units of the single particle estimate. This transition probability is obtained from Coulomb excitation results[65]. In the Coulomb excitation process the target nuclei are bombarded with charged particles whose energy is low enough so that

TABLE 2.   PROPERTIES OF EVEN-EVEN NUCLEI HAVING ASSIGNMENTS
OF 2^+ FOR BOTH THE FIRST AND SECOND EXCITED STATES

Nucleus	E_2 (Mev)	$E_{2'}$ (Mev)	$E_{2'}/E_2$	$\dfrac{B(E2;\ 0\to 2)}{B_{sp}(E2)}$	$(M1/E2)_{2'\to 2}$	$\dfrac{B(E2;\ 2'\to 0)}{B(E2;\ 2'\to 2)}$
$_{26}Fe^{58}$	0.81	1.62	2.00		0.2	0.01
$_{28}Ni^{60}$	1.33	2.18	1.64	17		(3.10^{-3})
$_{30}Zn^{64}$	1.00	2.27	2.27	15		(0.1)
Zn^{66}	1.05	2.40	2.29	11		(0.04)
$_{34}Se^{76}$	0.55	1.19	2.17	45	~ 1	0.1
$_{36}Kr^{82}$	0.77	1.45	1.88			(0.01)
Kr^{84}	0.9	1.9	2.1			>0.1
$_{40}Zr^{92}$	0.93	1.83	1.97			(0.06)
$_{44}Ru^{100}$	0.54	1.36	2.52	22		(0.02)
Ru^{102}	0.47	1.10	2.34	45		(0.15)
$_{52}Te^{122}$	0.57	1.26	2.21	26	0.1	0.01
Te^{126}	0.65	1.40	2.16	17		(0.004)
$_{54}Xe^{126}$	0.39	0.86	2.20			(0.01)
Xe^{128}	0.46	0.98	2.13			(0.01)
$_{78}Pt^{192}$	0.32	0.61	1.90		0.025	0.008
Pt^{194}	0.33	0.62	1.88	50	small	0.01
Pt^{196}	0.35	0.69	1.97	38	0.05	$< 4.10^{-4}$
$_{80}Hg^{198}$	0.41	1.09	2.66	29	0.7	0.03
$_{84}Po^{214}$	0.61	1.38	2.26	15	$\gtrsim 1$	

they will not penetrate the Coulomb barrier of the nucleus and cause a nuclear reaction. The electromagnetic field of the charged particle interacts with the nucleus and can cause a nuclear excitation. Coulomb excitation is mainly an electric quadrupole process. The yield function can be measured accurately and the cross section for E2 excitation calculated. From Table 2 it is seen that for all those nuclei whose first 2^+ state has been excited by Coulomb excitation, the observed cross section is greater than that expected for a single particle excitation.

The sixth column in Table 2 gives the ratio of M1 to E2 radiation in the $2^+ \rightarrow 2^+$ transition as determined from angular correlation or conversion coefficient data. It is seen that in almost all cases there is a large admixture of electric quadrupole radiation in the $2^+ \rightarrow 2^+$ transition.

The seventh column gives the ratio of the reduced E2 transition probabilities for the cross-over and cascade radiation from the second excited state. The reduced transition probability $B(L; I_f \rightarrow I_i)$ is defined in terms of the total transition probability T by the expression[65]

$$T = \frac{8\pi (L+1)}{L [(2L+1)!!]^2} \frac{1}{\hbar} \left(\frac{\omega}{c}\right)^{2L+1} B(L; I_f \rightarrow I_i)$$

where L is the multipolarity and ω is the angular frequency of the radiation ($\omega = E/\hbar$). It is seen from Table 2 that the reduced transition probability for the cross-over transition is considerably less than that for the cascade decay for all cases listed. On the basis of a single particle model they would be approximately equal.

The results presented in Table 2 indicate that the excitations involved here are due mainly to a cooperative motion involving many

nucleons. It is known that nuclei with doubly closed shells have very high binding energies and are spherically symmetric. Nuclei which have many particles in unfilled shells exhibit large quadrupole moments and nuclear spectra which can be explained by a collective rotation of the nucleons about a non-spherical equilibrium shape, the so-called rotational spectra. In the intermediate regions between these extremes, excited states corresponding to quadrupole vibrations (ellipsoidal vibrations) about a spherical equilibrium shape might be expected[65,66]. An enhancement of E2 transition probabilities would then be associated with these vibrational states.

The characterization of excitation level spectra as vibrational is not expected to be as accurate as in the case of rotational spectra. The vibrational energies involved (several hundred kev to 1 Mev) are no longer very small compared to typical intrinsic particle excitation energies (1 or 2 Mev), and therefore interaction between the intrinsic motion and the vibrational motion may be significant. In the case of rotational spectra, the rotational energies are much smaller than the intrinsic excitation energies, and coupling between the two is insignificant for the low-lying levels.

The shape oscillations of a spherical nucleus can be classified according to their multipole order λ[66]. The excitation quanta are called phonons and have total angular momentum λ and parity $(-1)^{\lambda}$. The vibrational motion is associated with an oscillating electric multipole moment. For small amplitudes of oscillation (e.g., harmonic deformation potential) the solution of the Schrodinger equation gives a harmonic energy spectrum with a uniform spacing between the levels. The lowest frequencies of collective vibration are expected to be of quad-

rupole type (λ = 2) since a surface deformation with λ = 1 merely represents a center-of-mass displacement.

The vibrational excitation spectra are simplest for the ground-state configuration of even-even nuclei for which the intrinsic structure does not contribute to the nuclear angular momentum. The energy spectrum assuming harmonic vibrations is shown up to the 2 phonon state in Figure 12a.[66]. A state of energy $E^{(n)}$ = (n + 5/2) $\hbar\omega_2$ can be characterized as containing n phonons each of which carries an angular momentum of 2 and even parity. Therefore all the excited states have even parity. The second excited state is degenerate with spins 0^+, 2^+, and 4^+ in the harmonic approximation. E2 transitions between the 2 $\hbar\omega_2$ state and the ground state are forbidden since the phonon number cannot change by more than one, and M1 transitions between any pair of levels are forbidden in this simple model for even-even nuclei.

For the group of nuclei considered in Table 2 the ratios of the energies of the second and first excited states are rather close to 2 which suggests that the harmonic approximation has some validity. The large electric quadrupole admixture in the transition from the second to the first excited state and the fact that the crossover transition is inhibited in these nuclei give additional support to this model.

Calculations have also been made assuming an anharmonic deformation potential[67]. The potential is assumed to be a function only of a quantity β which measures the deviation from sphericity of the nucleus. The potential is not dependent on the specific shape of the nucleus (i.e., no favoring of prolate or oblate shapes). According to these calculations the degeneracy of the second excited state is partially lifted, but the 2^+ and 4^+ states remain at the same energy. This is shown in Figure 12b.

a. Harmonic   b. Anharmonic   c. Experimental

$2\hbar\omega_2$———————$0,2,4^+$ ———————0^+

                                                                  ———————4^+

                                       ———————$2,4^+$

                                                                  ———————2^+

$1\hbar\omega_2$————————2^+

                                       ————————2^+ ————————2^+

$0\hbar\omega_2$————————0^+ ————————0^+ ————————0^+
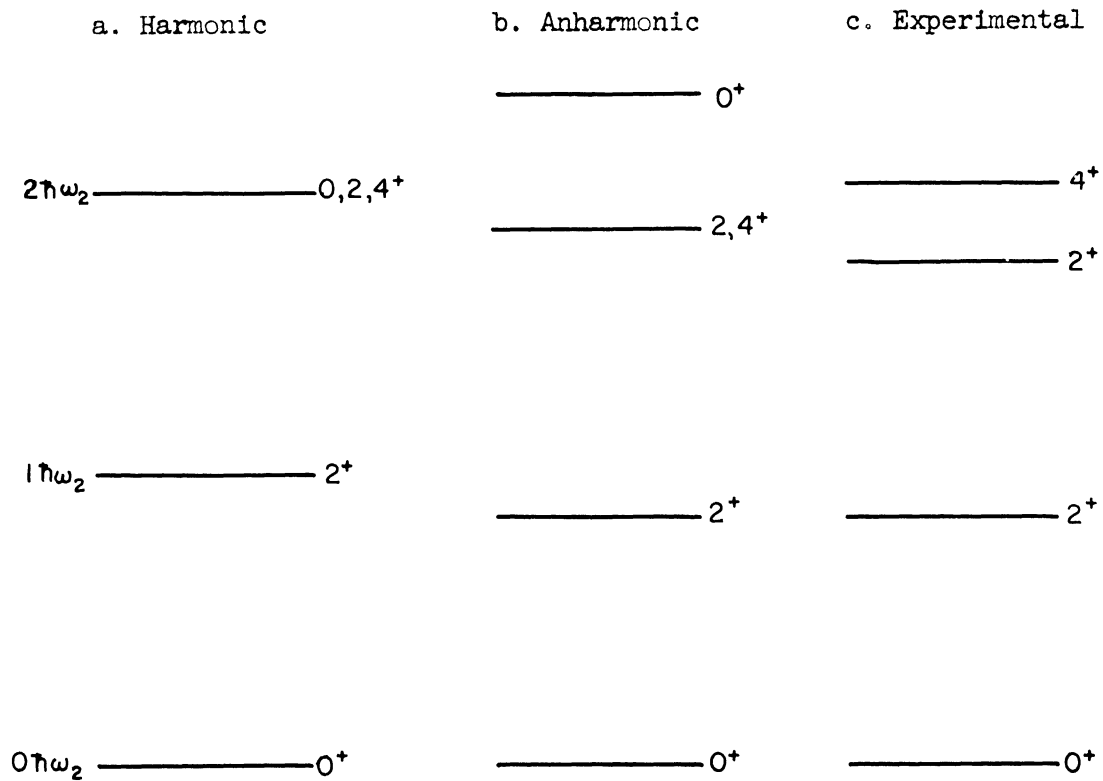
Figure 12. Vibrational Spectra in Even-Even Nuclei

The E2 crossover transition between the second 2^+ state and the ground state is still expected to remain forbidden. The ratio of the energies of the second and first excited states is now expected to be slightly larger than 2. The average value 2.2 of the empirical ratio implies that there is actually some anharmonicity but with the spherical shape at least on the borderline of being stable. Any favoring of prolate or oblate shapes will split the degeneracy between the 2^+ and 4^+ states but always so as to lower the 4^+ state if there is no vibration-particle coupling. The frequent appearance of 2^+ second excited states, Figure 12c, may be due to coupling between the vibrational motion and the intrinsic

particle motion. This effect could be important since the vibrational energies are not much smaller than the excitation energies of the individual nucleons.

The theory of vibrational spectra has been somewhat successful in explaining the character of the first few excited states in several of the nuclei listed in Table 2. However, more theoretical work must be done, especially in the case of higher excited states where vibration-particle coupling becomes important.

An explanation of the Se^{76} level scheme in terms of vibrational levels presents some interesting problems. The Se^{76} nucleus contains 34 protons and 42 neutrons. Therefore Se^{76} has 6 protons outside of the partially closed proton shell at Z = 28 and 8 neutrons lacking from the closed neutron shell at N = 50, and it might be expected to exhibit a vibrational level structure. The first excited state in Se^{76} has been reached by Coulomb excitation,[68] and the cross-section for this was found to be much larger than the cross-section expected for a single particle excitation (Table 2). The Coulomb excitation result, the value of 2.17 for the ratio $E_{2'}/E_2$, the fact that the 0.65 Mev gamma transition is almost pure E2, and the inhibition of the 1.20 Mev crossover transition, (Table 2) all suggest that the first two excited states are mainly vibrational in character. Therefore it is concluded that the first excited state is mainly the result of a one-phonon vibrational excitation while the second excited state is mainly the result of a two-phonon vibrational excitation. Since the 0.65 Mev gamma transition contains some M1 radiation and the 1.20 Mev cross-over transition is not completely forbidden, it must be assumed that the second excited state is not a pure vibrational state but that some vibration-particle coupling exists.

The very different nature of the two transitions originating from the third excited state in Se^{76} is difficult to understand. One possibility is that the third excited state is due to a two-phonon vibrational excitation coupled with a single particle excitation of the ground state configuration. If this is true, then the 1.40 Mev gamma ray occurs between two states with the same number of phonons and is primarily a single particle transition. This could account for the fact that the 1.40 Mev gamma transition is almost pure magnetic dipole radiation. However, the 2.05 Mev transition would require both a change in vibrational excitation and particle excitation, and this might account for the large E2 component ($\sim 95\%$) in the 2.05 Mev transition.

CHAPTER V

RESULTS OF GAMMA-GAMMA DIRECTIONAL CORRELATION MEASUREMENTS IN Cd^{110}

Introduction

Ag^{110m} decays by complex beta emission to excited states of Cd^{110} and by an isomeric gamma transition to the ground state of Ag^{110} with a half-life of 253 days[69]. Ag^{110} in turn decays to Cd^{110} by complex beta emission with a half-life of 24 seconds. The decay of Ag^{110m} has been the subject of numerous investigations[70-76].

The presently accepted decay scheme, which was first proposed by Siegbahn[70], is shown in Figure 13. The relative gamma intensities (in parentheses) and energy values are due to Siegbahn[70]. The gamma rays for which no intensities are given are weak transitions. The position of the 656 kev, 885 kev, 935 kev and 1389 kev gamma rays in the scheme has been well established by coincidence measurements[70,74]. The 1516 kev gamma is known to be in coincidence with the 759 kev and 656 kev gammas, but the order of the 1516 kev and 659 kev gamma transitions has not been definitely established. Siegbahn placed them in the order shown in Figure 13 on the basis of the estimated relative intensities and the fact that the three weak gammas with energies of 706 kev, 676 kev, and 814 kev could then be fitted in with the addition of only one more level. Four additional weak gamma rays have been found in conversion electron work. These are at 575 kev[76], 618 kev[71,75,76], 740 kev[71] and 1480 kev[71,76]. However, these cannot be fitted into the previous decay scheme.

The K-shell internal conversion coefficient for the 656 kev transition has been measured by Siegbahn to be $(2.5 \pm 0.4) \times 10^{-3}$. The theoretical values obtained by interpolation from Sliv and Bands' tables
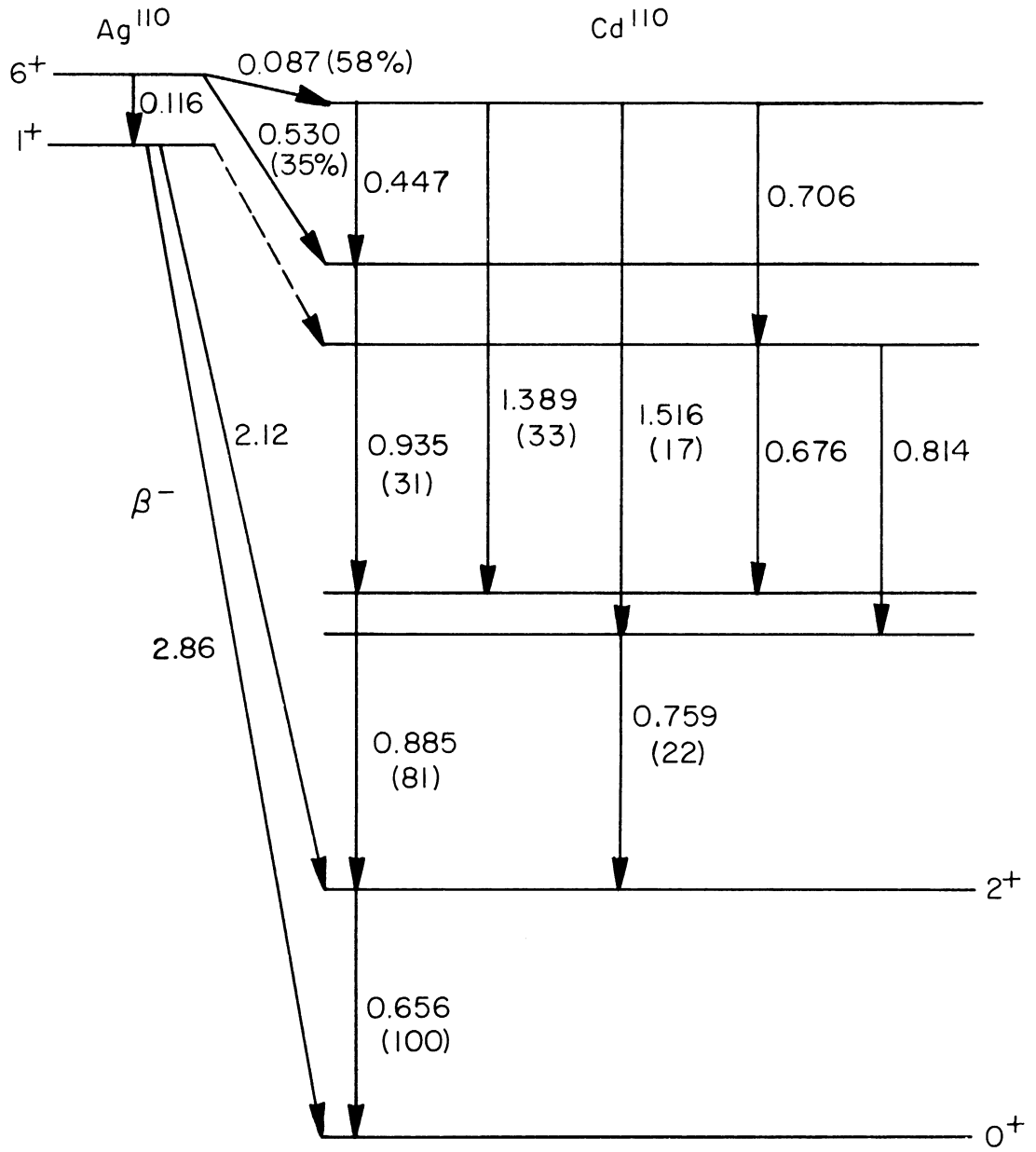
Figure 13. Decay Scheme of Ag[110m]

of α_K[77] are 1.0 x 10^{-3} for E1, 2.75 x 10^{-3} for E2 and 3.1 x 10^{-3} for

M1 radiation. The experimental value agrees best with an assignment of

E2 for the 656 kev gamma ray. Assuming 0^+ for the ground state of the

even-even nucleus Cd^{110}, the first excited state is then 2^+. The fact that

the first excited state has been Coulomb excited[78,79] supports this

assignment.

Measurements of K/(L+M) ratios have been made for many of the

gamma transitions[71]. However, no information concerning multipolarities

can be learned from these because the theoretical K/(L+M) ratios are very

insensitive to multipole order in this region of Z and for the energy

values involved.

The beta spectrum of Ag^{110m} has been investigated by several

groups[70-76]. Two high energy beta transitions of allowed type with

endpoint energies of 2.86 Mev and 2.12 Mev have been found. These origin-

ate from the ground state of Ag^{110} and go to the ground state and first

excited state of Cd^{110}. Since both transitions are of allowed type[80]

(ΔJ = 0 or $\pm$ 1, no) the spin of the ground state of Ag^{110} must be 1^+.

This agrees with the value predicted by Nordheim's rules[59]. Antoneva[71]

has reported an additional weak group at about 1.4 Mev, but no confirmation

of this has been made. Two soft beta transitions with endpoint energies

of 87 kev and 530 kev originate from Ag^{110m}. The Fermi plot of the 530 kev

beta has been reported to be curvilinear, and Siegbahn[70] suggested that

another weak low energy group might be present (dotted line in Figure 13).

It is possible, however, that the 530 kev beta transition is of forbidden

type which would give a non-linear Fermi plot.

Using the measured beta branching ratios[71], approximate log

ft values for the low energy beta transitions can be found from Moszkowski's

graphs[81]. This gives a log ft value of about 8.4 for the 530 kev beta and about 5.6 for the 87 kev beta. These values indicate that the 530 kev beta is a forbidden transition while the 87 kev beta is of allowed type.

The spin of Ag^{110m} has been measured recently by an atomic beam method, and a value of 6 was found[82]. Since the ground state spin is 1^+, the 116 kev isomeric transition must then be either M5 or E5 radiation. The K/(L+M) and K/L ratios for the highly converted 116 kev gamma transition have been measured by several groups[70,71,75,76]. Siegbahn[70] reported a K/L value of 1.3 which is close to the theoretical value of 1.2 for an M5 transition. The theoretical value for an E5 transition is 0.24. All other measurements gave K/(L+M) values between 1.2 and 2.1. Thus it is concluded that the 116 kev gamma is an M5 transition, and consequently the Ag^{110m} level must have positive parity.

Even though the decay scheme is quite complex, which makes correlation work difficult, any correlation measurements would be useful in determining the spins of the levels in Cd^{110}. The following directional correlation measurements are proposed:

1.389 Mev - 0.885 Mev, 0.935 Mev - 0.885 Mev, 0.885 Mev - 0.656 Mev, 1.516 Mev - 0.759 Mev, 1.516 Mev - 0.656 Mev and 1.389 Mev - 0.656 Mev. The source material was obtained from Oak Ridge. It was in the form of $AgNO_3$ in HNO_3. No appreciable contamination was present in the source. The mean lifetime of the first excited state has been measured to be about 5.5×10^{-12} sec.[78,79] and the other intermediate state lifetimes are assumed to be small. Because of this and the fact that the source was in a dilute solution, the correlations should not be attenuated due to extranuclear fields. The observed scintillation spectrum is shown in Figure 14.
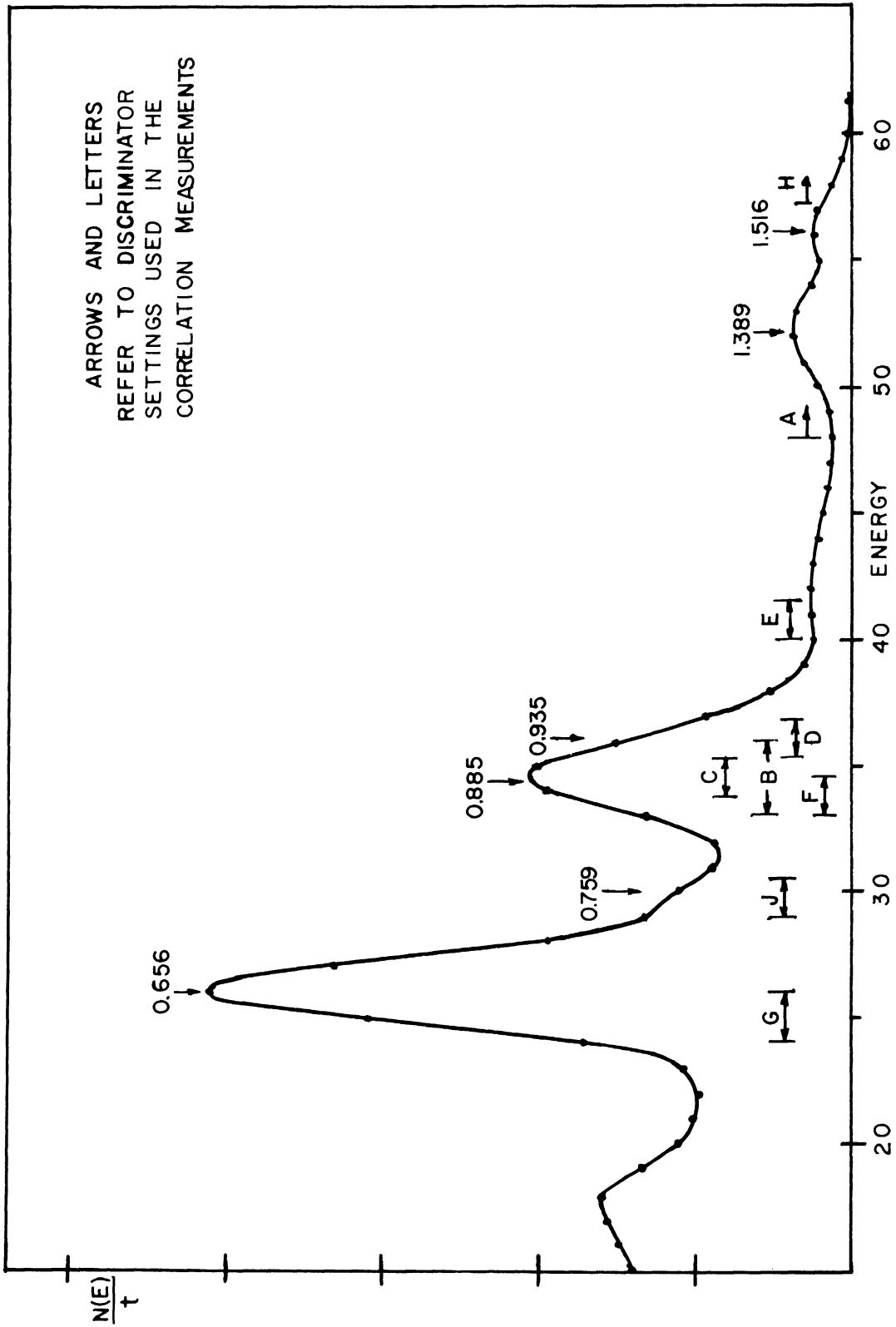
Figure 14. Scintillation Spectrum of Gamma Rays of Cd^{110}

Results

1.389 Mev - 0.885 Mev Directional Correlation

For the 1.389 Mev - 0.885 Mev correlation one discriminator was set integrally at position A and the other differentially at position B as shown in Figure 14. With these settings there is no interference from any other cascades, and the full correlation is expected. Lateral lead shielding was not needed for this correlation since coincidences due to scattering were eliminated by energy selection. The least squares curve corrected for finite geometry is shown in Figure 15. The error flags represent the root-mean-square statistical errors of the experimental points. The corrected correlation function shows an asymmetry of 39% negative. (Asymmetry is defined as $A = \dfrac{W(180°) - W(90°)}{W(90°)}$.) The correlation function is given by

$$W(\theta) = 1 - (0.308 \pm 0.013) \, P_2(\cos \theta) + (0.009 \pm 0.020) \, P_4(\cos \theta)$$

0.935 Mev - 0.885 Mev Directional Correlation

Since the 1.389 Mev and 0.935 Mev gamma rays are of comparable intensity, the 0.935 Mev - 0.885 Mev correlation cannot be done without interference from the 1.389 Mev - 0.885 Mev correlation. Because the 1.389 Mev - 0.885 Mev correlation has a large asymmetry, the interference can cause the observed 0.935 - 0.885 correlation to be quite different from the true correlation. In this case, however, a fairly accurate subtraction process can be carried out to eliminate the interference. This was done in the following manner. First, discriminator I was set differentially on the 885 kev peak and discriminator II differentially at the position where the 935 kev peak is expected (C and D in Figure 14). The correlation was then run at all angles and the total real coincidence
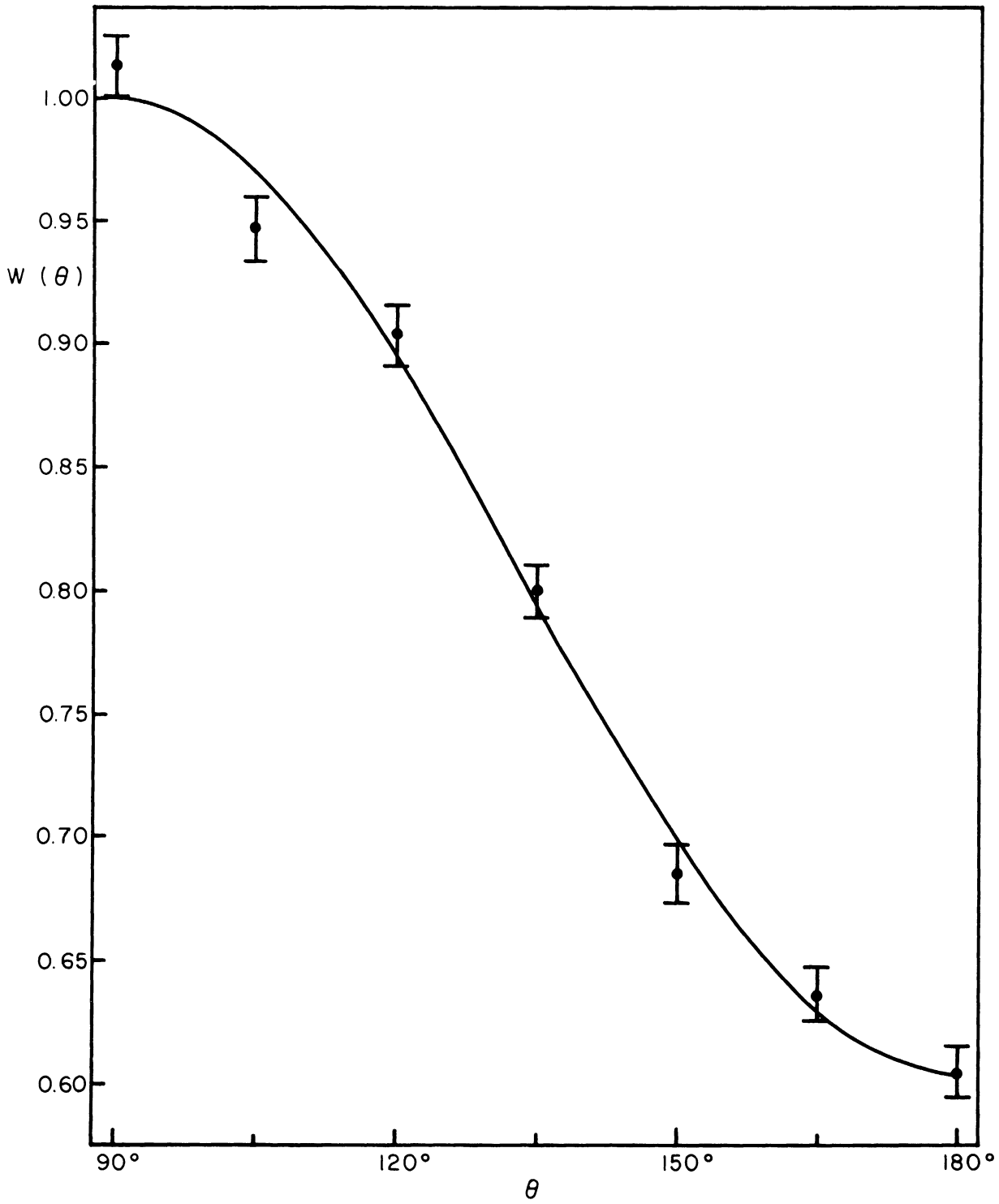
Figure 15.   1.389 Mev - 0.885 Mev Correlation in Cd^{110}

rates $N_R(\theta_i)$ were found. For the second measurement, discriminator I was set differentially (with the same discriminator window as previously) on the Compton distribution of the 1.389 Mev gamma (position E in Figure 14) and discriminator II was left on the 935 kev peak (position D). Data were taken at just the 90° and 180° points and the total real coincidence rates $N_R^{(2)}$ (90°) and $N_R^{(2)}$ (180°) were found. For the third measurement, discriminator I was set back on the 885 kev peak as in the first measurement and discriminator II was set differentially (with the same window as previously) on the 1.389 Mev Compton distribution (position E). Data were taken at the 90° and 180° points, giving the total real coincidence rates $N_R^{(3)}$(90°) and $N_R^{(3)}$(180°). As expected, the asymmetry observed in measurements 2 and 3 was approximately the same as that found in the measurement of the 1.389 Mev - 0.885 Mev correlation. In all three measurements lateral lead shielding was used to eliminate coincidences due to scattering. The coincidence rates $N_R^{(2)}$(90°) and $N_R^{(3)}$(90°) were added together giving the total background coincidence rate at 90°, N_B(90°). The background coincidence rate at each angle $N_B(\theta_i)$ was found by multiplying N_B(90°) by the value of $W(\theta_i)$ for the 1.389 Mev - 0.885 Mev interfering correlation (after $W(\theta_i)$ was normalized to 1 at 90°). The 0.935 Mev - 0.885 Mev coincidence rates were then found by subtracting $N_B(\theta_i)$ from the corresponding $N_R(\theta_i)$. Since some uncertainty was obviously introduced here, a $\pm$ 10% error was assigned to the background coincidence rates before subtraction.

One important assumption must be made in this process. That is, the Compton distribution of the 1.389 Mev gamma ray is assumed to be flat below the Compton peak. This is quite valid for the type of crystals and geometry employed in the measurements.

The 0.935 Mev - 0.885 Mev correlation function after correction for the background correlation and finite geometry is shown in Figure 16. The correlation function before correction for the background has an asymmetry of about 7% positive, while the corrected correlation function shows an asymmetry of about 23% positive and is given by

$$W(\theta) = 1 + (0.150 \pm 0.027) \ P_2(\text{Cos } \theta) - (0.006 \pm 0.036) \ P_4(\text{Cos } \theta)$$

0.885 Mev - 0.656 Mev Directional Correlation

For this correlation one discriminator was set differentially on the low energy side of the 0.885 Mev peak and the other differentially on the low energy side of the 0.656 Mev peak (positions F and G in Figure 14). Lateral lead shielding was used. Even though the 0.885 Mev and 0.656 Mev gamma rays are the most intense gammas in the decay, some interference will be present from the other cascades. Since some of the interfering correlations have positive asymmetries and some have negative asymmetries, the net effect is probably a fairly isotropic interference which will lower the whole correlation somewhat. With the discriminator settings used, it is estimated that about 10% of the total coincidence counts are due to interfering cascades. However, no correction for this was made because of the uncertainty involved.

The least-squares curve corrected for finite geometry is shown in Figure 17. The correlation function shows a 12% positive asymmetry and is given by

$$W(\theta) = 1 + (0.073 \pm 0.014) \ P_2(\text{Cos } \theta) + (0.009 \pm 0.020) \ P_4(\text{Cos } \theta)$$

If a 10% isotropic background were present, the asymmetry in the correlation function would be about 14%.

1.516 Mev - 0.656 Mev and 1.516 Mev - 0.759 Mev Directional Correlations

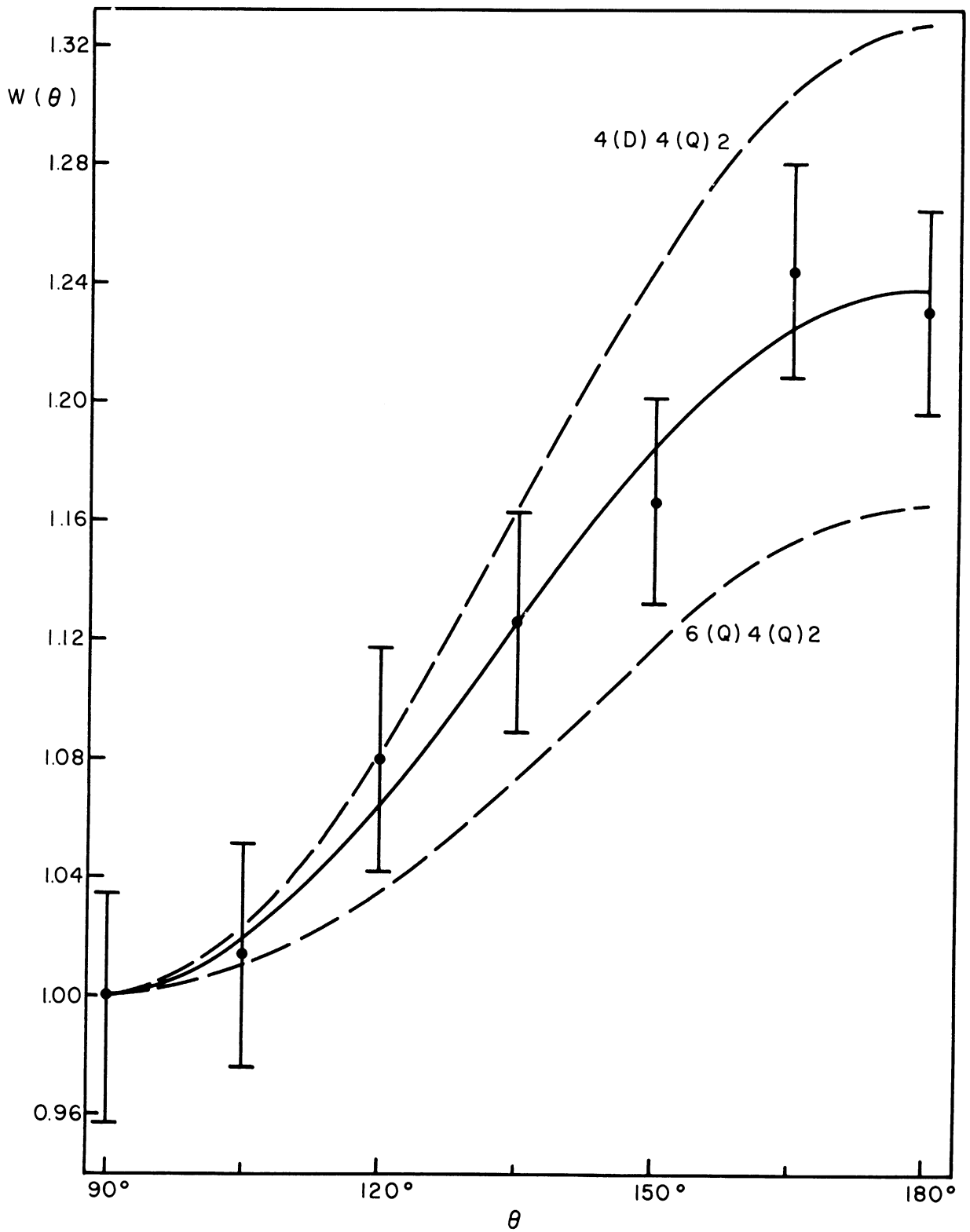The 1.516 Mev - 0.656 Mev and 1.516 Mev - 0.759 Mev correlations

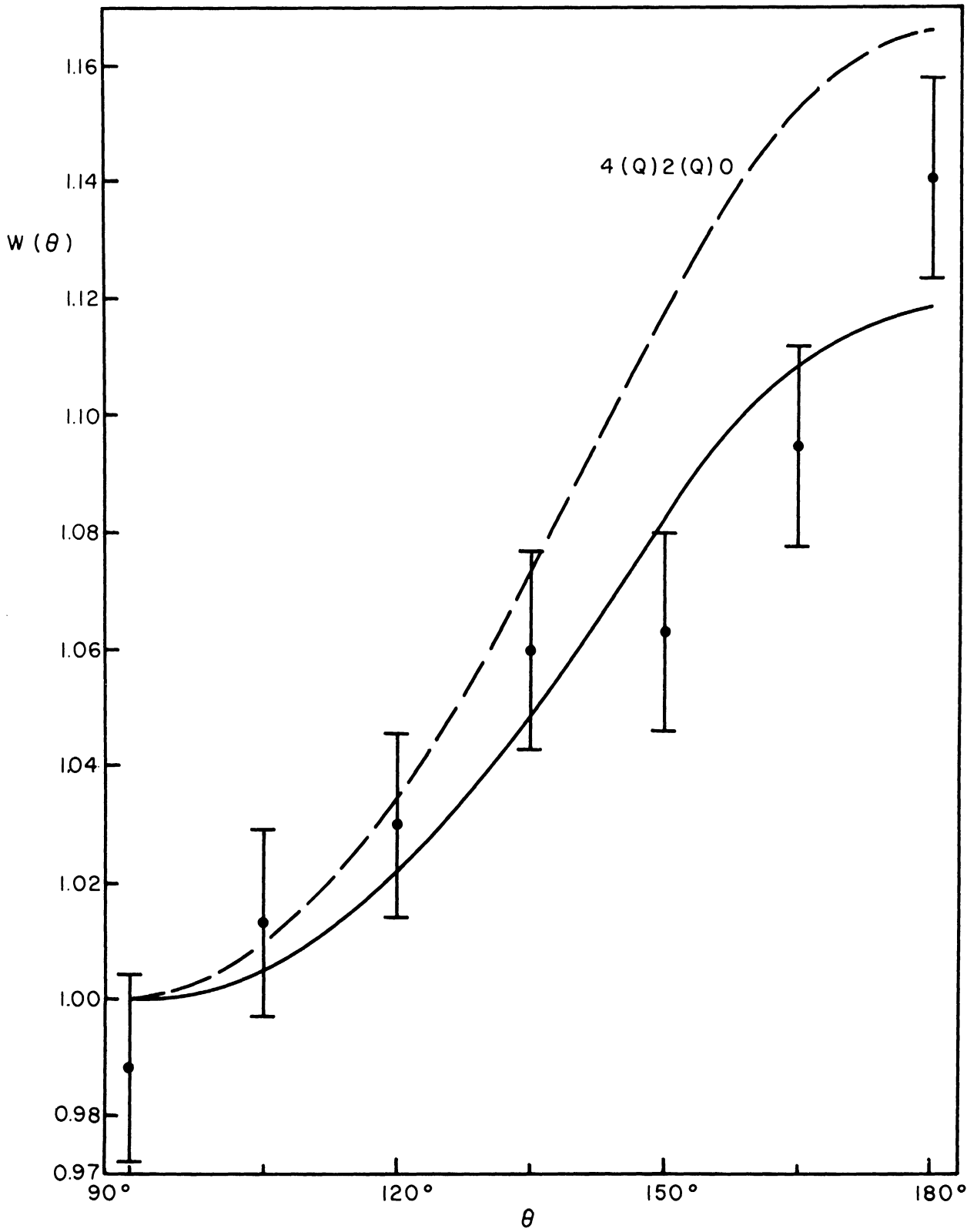Figure 16.   0.935 Mev - 0.885 Mev Correlation in Cd^{110}

Figure 17. 0.885 Mev - 0.656 Mev Correlation in Cd^{110}

are complicated by the fact that the 0.656 and 0.759 peaks are not re-solved by the scintillation counters. In addition, the 1.516 and 1.389 peaks are only partially resolved. However, because the 1.516 peak lies above the 1.389 peak, an effective selection of the 1.516 gamma of about 80% can be attained. To circumvent the first problem, the following pro-cedure was followed.

(a) Discriminator I was set integrally on the high energy side of the 1.516 Mev peak (position H in Figure 14) and discriminator II was set differentially on the 0.759 Mev peak (position J). No lateral lead shielding was needed here. The correlation was run at all seven angles giving the corrected correlation function $W_a(\theta)$ where

$$W_a(\theta) = 1 - (0.202 \pm 0.021) \, P_2(\cos \theta) - (0.006 \pm 0.030) \, P_4(\cos \theta)$$

The correlation function $W_a(\theta)$ is mainly composed of the 1.516 - 0.759 correlation but contains some interference from the 1.516 - 0.656 correlation. It is shown as curve a in Figure 18.

(b) Discriminator I was left at the same setting while dis-criminator II was set differentially on the low energy side of the 0.656 peak (position G). For this case the corrected correlation function was given by

$$W_b(\theta) = 1 - (0.328 \pm 0.023) \, P_2(\cos \theta) - (0.022 \pm 0.031) \, P_4(\cos \theta)$$

The correlation function $W_b(\theta)$ is mainly composed of the 1.516 - 0.656 correlation but contains some interference from the 1.516 - 0.759 correlation. It is shown as curve b in Figure 18.

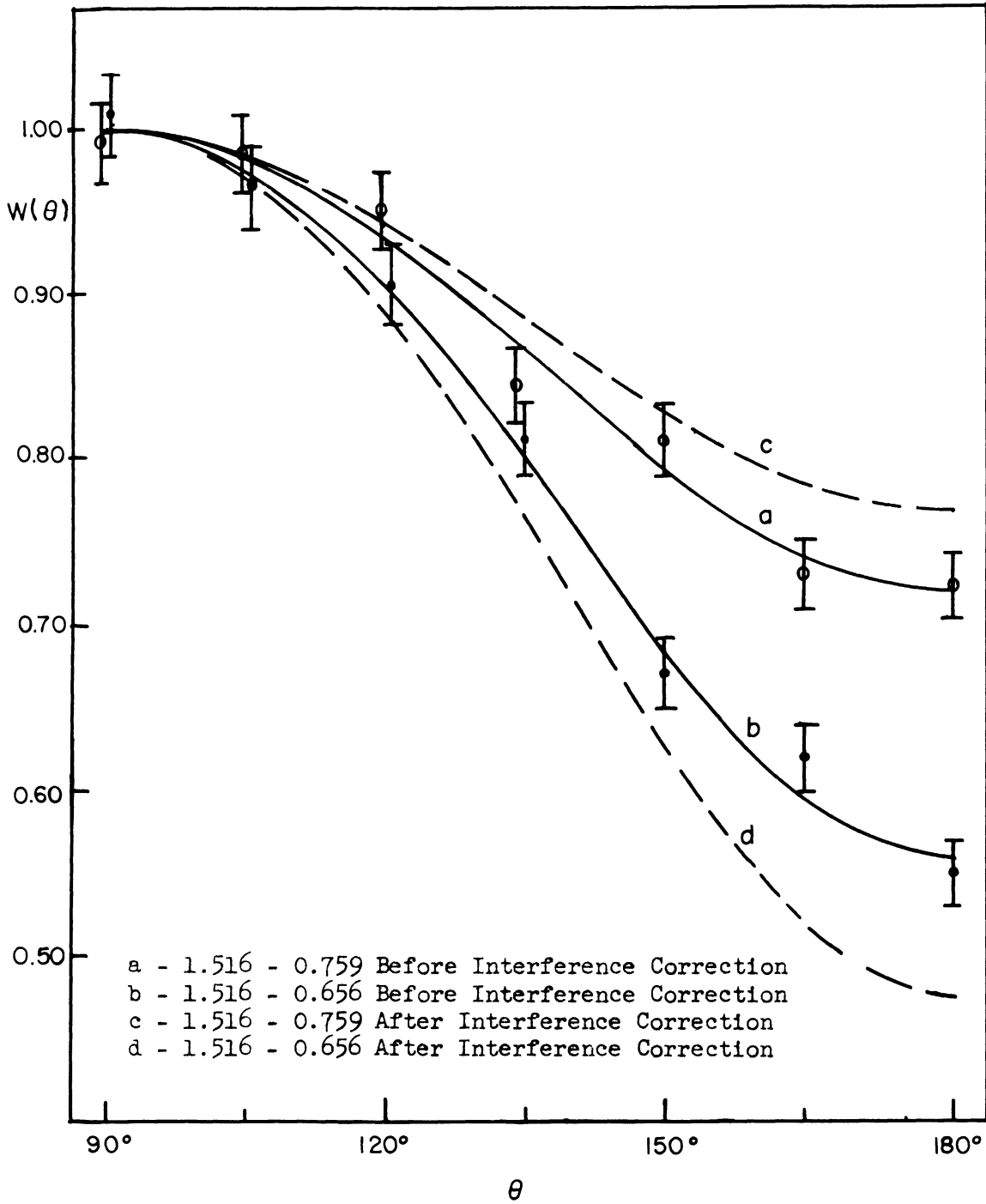If $W_1(\theta)$ is the true 1.516 - 0.759 correlation function, and

Figure 18. 1.516 Mev - 0.759 Mev and 1.516 Mev - 0.656 Mev
Correlations in Cd^{110}

$W_2(\theta)$ is the true 1.516 - 0.656 correlation function, then the observed correlations W_a and W_b are given by

$$W_a = X_a W_1 + (1-X_a)W_2 \tag{23}$$

$$W_b = X_b W_1 + (1-X_b)W_2 \tag{24}$$

where X_a and X_b are the fractions of W_a and W_b composed of the 1.516 - 0.759 correlation. Solving these equations for W_1 and W_2 one obtains

$$W_1 = \frac{(1-X_b)W_a - (1-X_a)W_b}{X_a-X_b} \tag{25}$$

$$W_2 = \frac{X_a W_b - X_b W_a}{X_a-X_b}$$

To correct for the interference, the quantities X_a and X_b must be determined.

X_a and X_b were found in the following manner. First, the scintillation spectrum of Cs^{137} was run using about the same source strength as the Ag^{110m} source. Cs^{137} contains a single gamma ray at 662 kev. Using the Cs^{137} spectrum, the individual 656 kev and 759 kev Cd^{110} peaks were constructed graphically, assuming equal intensity for both peaks. The areas under the peaks corresponding to the discriminator settings in a and b were then determined. This gave approximate values for the quantities X_a and X_b.

The values found were $X_a = 0.85$ and $X_b = 0.32$. Since some uncertainty is introduced here, it was considered reasonable to assign maximum errors of $\pm$ 0.10 to X_a and X_b. Therefore values of X_a from 0.75 to 0.95 and values of X_b from 0.22 to 0.32 were considered in the calculation of the correlation functions W_1 and W_2 from Equations (25) and (26).

The result for the 1.516 Mev - 0.759 Mev correlation function

was

$$W_1(\theta) = 1 - (0.166^{+0.050}_{-0.100})P_2(\cos \theta) - (0.002^{+0.035}_{-0.066})P_4(\cos \theta)$$

and the result for the 1.516 Mev - 0.656 Mev correlation function was

$$W_2(\theta) = 1 - (0.404^{+0.135}_{-0.070})P_2(\cos \theta) - (0.031^{+0.091}_{-0.045})P_4(\cos \theta)$$

The coefficients in W_1 and W_2 are the values found for $X_a = 0.85$ and

$X_b = 0.32$. The errors quoted for the coefficients correspond to the

maximum errors assigned to X_a and X_b. These correlation functions are shown

as curves c and d in Figure 18.

1.389 Mev - 0.656 Mev Directional Correlation

For this correlation, one discriminator was set integrally below

the 1.389 Mev and 1.516 Mev peaks (position A in Figure 14) and the other

discriminator differentially on the low energy side of the 0.656 Mev peak

(position G). This correlation consisted mainly of a composite of the

1.516 - 0.656 and 1.389 - 0.656 correlations and showed an asymmetry of

40% negative. A least squares analysis of the data was not made because

of the difficulty involved in interpreting the coefficients due to the

interfering cascades. It was estimated that about 45% of the coincidences

were due to the 1.389 - 0.656 correlation and about 25% were due to the

1.516 - 0.656 cascade. Other interfering cascades were the 1.516 - 0.760

($\sim$10%) and 1.389 - 0.885 ($\sim$20%). Assuming these rough estimates for

the interference, and the asymmetries measured previously for the inter-

fering correlations, it was concluded that the 1.389 Mev - 0.656 Mev cor-

relation has an asymmetry of about 40% negative.

Interpretation of Results

To facilitate the interpretation of the correlation results the experimental values of A_2 and A_4 are summarized in Table 3.

TABLE 3.   DIRECTIONAL CORRELATION RESULTS FOR Cd^{110}

Correlation	A_2	A_4
1.389-0.885	- 0.308+0.013	0.009+0.020
0.885-0.656	0.073+0.014	0.009+0.020
0.935-0.885	0.150+0.027	- 0.006+0.036
1.516-0.759	$-(0.166^{+0.050}_{-0.100})$	$-(0.002^{+0.035}_{-0.066})$
1.516-0.756	$-(0.404^{+0.135}_{-0.070})$	$-(0.031^{+0.091}_{-0.045})$
1.389-0.656	Asymmetry $\sim$ -0.40	

The portion of the decay scheme which is pertinent to the data taken is shown in Figure 19, and the possible spins which must be considered for each level are listed. The levels are designated by Roman numerals and henceforth will be referred to by these numbers. The possible spin values are arrived at by considering the beta decay data, the relative gamma intensities, and the known spin values for the Ag^{110} levels and the two lowest Cd^{110} levels. Because of the nature of the beta transitions to levels V and VI, the only spin values which must be considered for these two states are 4, 5 and 6. Since no cross-over transitions from states III and IV to the ground state have been observed and no beta transitions leading to levels III and IV have been found, no spin lower than 2 or higher than 4 need be considered for levels III and IV.
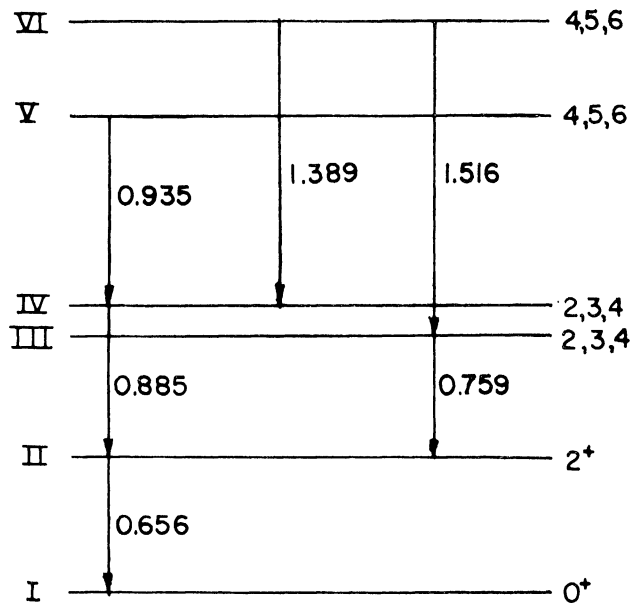
Figure 19. Main Portion of Cd^{110} Level Scheme

Interpretation of 1.389 Mev - 0.885 Mev, 0.885 Mev - 0.656 Mev, and 1.389 Mev - 0.656 Mev Correlations

Since the 1.389 Mev - 0.885 Mev correlation is free of interference from other cascades it is the logical correlation with which to begin the interpretation. However, any spin value which is determined for level IV on the basis of the 1.389 - 0.885 correlation must also be consistent with the data from the 0.885 - 0.656, 0.935 - 0.885 and 1.389 - 0.656 correlations. These correlations provide a cross-check on the interpretation. Considering pure radiations only, no combination of the possible spins for levels II, IV and VI is consistent with the 1.389 Mev - 0.885 Mev data. If one considers dipole-quadrupole mixtures in one or both of the transitions, ohly three sequences are consistent with the data. These are 5(D,Q)4(Q)2, 6(0)3(D,Q)2 and 4(D,Q)3(D,Q)2. Since no sequence with a spin of 2 for level IV comes close to fitting the data, this spin value can be discarded. In Figure 20 the theoretical values for A$_2$ and A$_4$ are plotted

Figure 20. A_2 and A_4 vs. Q for a 5(D,Q)4(Q)2 Sequence

versus Q, the quadrupole content of the 5-4 transition, for the $5(D,Q)4(Q)2$
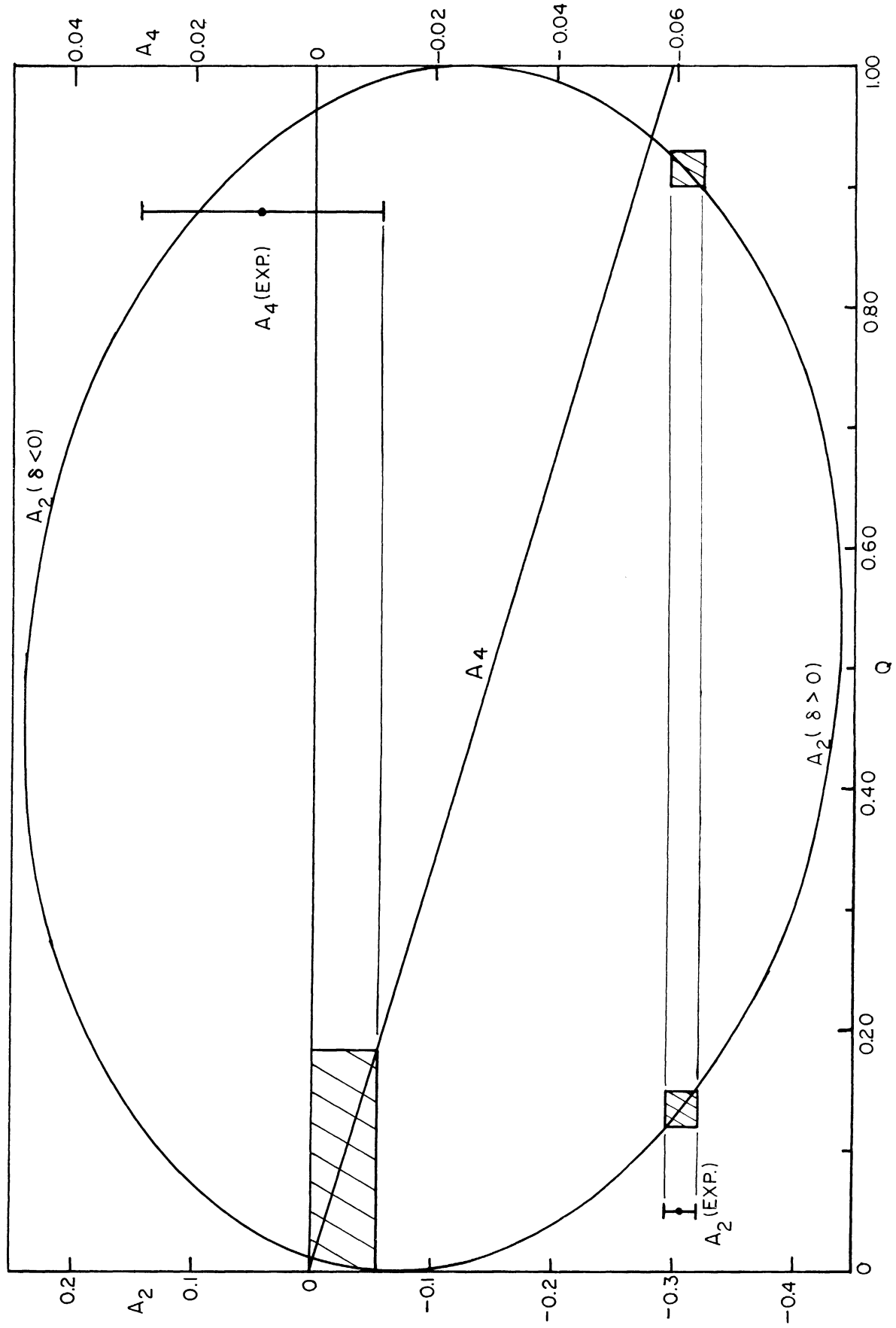
sequence. It is determined from Figure 20 that the experimental values of

A_2 and A_4 are consistent with a value of $Q = 0.135 \pm 0.015$ ($\delta > 0$). In

Figure 21 a similar curve is shown for a $6(0)3(D,Q)2$ sequence where Q is

the quadrupole content of the 3-2 transition. The data are consistent

with a value of $Q = 0.09 \pm 0.02$ or 0.73 ± 0.03 ($\delta < 0$).

The only spin values remaining for level IV are 3 and 4. Thus

it should be possible to explain the 0.885 Mev - 0.656 Mev correlation

by either a $4(Q)2(Q)0$ or $3(D,Q)2(Q)0$ sequence. In Figure 17, which shows

the 0.885 Mev - 0.656 Mev correlation function, the theoretical curve for

a $4(Q)2(Q)0$ sequence is also plotted. The observed curve does not quite

fit the theoretical $4(Q)2(Q)0$ curve, but the expected presence of inter-

ference from the other cascades could explain the discrepancy. The theor-

etical values of A_2 and A_4 for a $4(Q)2(Q)0$ sequence are $A_2 = 0.1020$ and

$A_4 = 0.0091$ while the experimental values are $A_2 = 0.073 \pm 0.014$ and

$A_4 = 0.009 \pm 0.020$. When the error in A_2 is considered, the discrepancy

is not too great. On this basis it is concluded that the $4(Q)2(Q)0$ se-

quence is consistent with the data for the 0.885 - 0.656 correlation.

Therefore spins of 5, 4, 2 and 0 for levels VI, IV, II and I respectively

are in agreement with both the 1.389 Mev - 0.885 Mev and 0.885 Mev -

0.656 Mev correlations.

The 0.885 Mev - 0.656 Mev correlation data can also be explained

by a $3(D,Q)2(Q)0$ sequence. From Figure 22 it is seen that the data for

the 0.885 - 0.656 correlation are consistent with a value of $Q = 0.04 \pm$

0.01 ($\delta < 0$). It was shown previously that a $6(0)3(D,Q)2$ sequence will

explain the 1.389 Mev - 0.885 Mev correlation. If the true sequence of

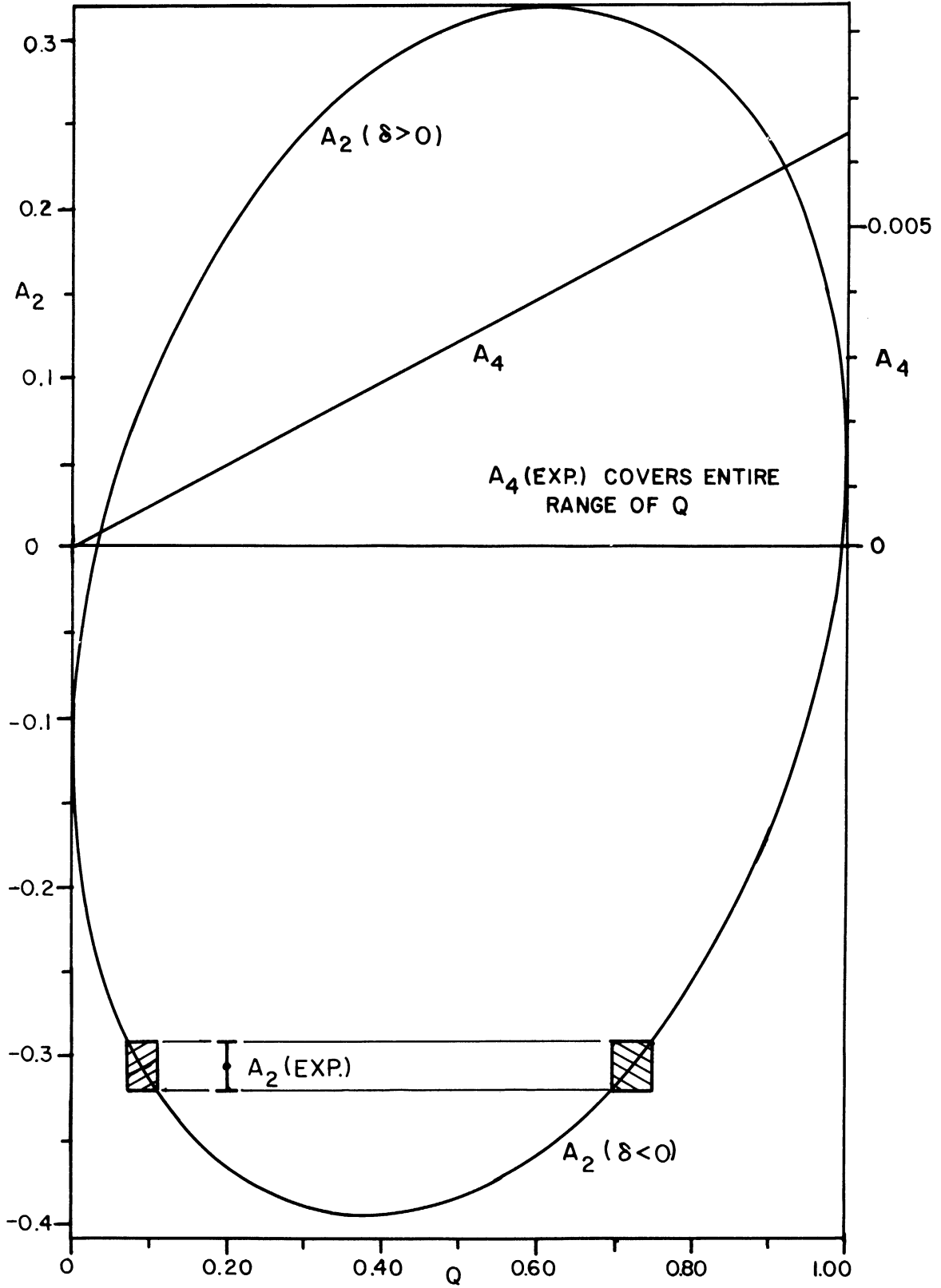spins is 6, 3, 2 and 0, the value of $Q = 0.04 \pm 0.01$ for the 0.885 Mev

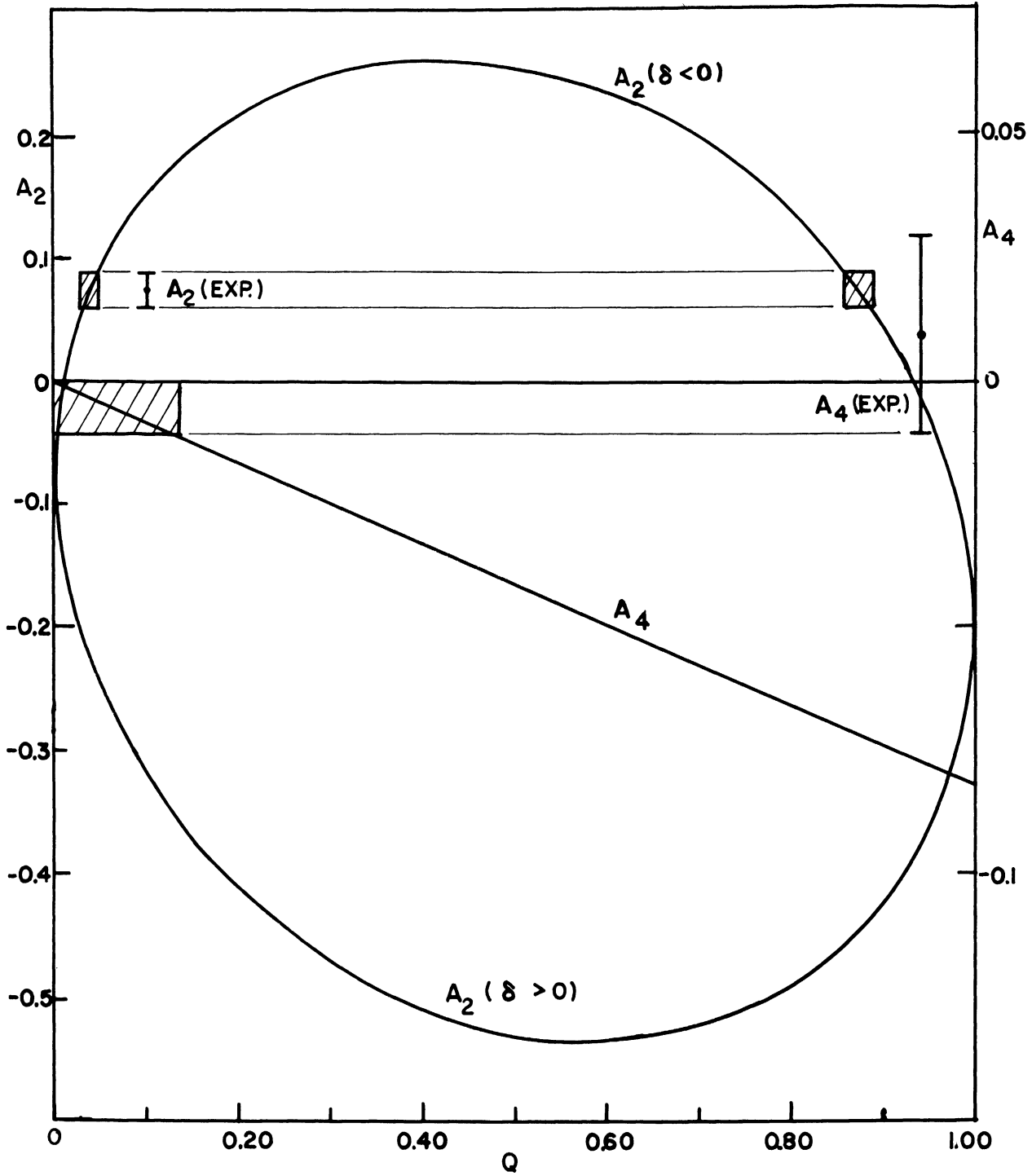Figure 21. A_2 and A_4 vs. Q for a $6(0)3(D,Q)2$ Sequence.

Figure 22. A_2 and A_4 vs. Q for a $3(D,Q)2(Q)0$ Sequence.

gamma as found from the 0.885 - 0.656 data should agree with the value

Q = 0.09 ± 0.02 found from the 1.389 - 0.885 data. There is a slight

discrepancy here. This can be explained easily if there is interference

present in the 0.885 - 0.656 correlation as mentioned before. If this is

considered, both correlations are then consistent with a value of Q =

0.09 ± 0.02 (δ< 0) for the 0.885 Mev transition.

It was stated previously that the 1.389 Mev - 0.885 Mev cor-

relation can also be explained by a 4(D,Q)3(D,Q)2 sequence (double mixture).

Assuming this sequence of spins, the mixing parameter for the 4-3 transi-

tion can be calculated using the value of Q = 0.04 ± 0.01 (δ< 0) for the

3-2 transition as found from the 0.885 - 0.656 correlation data. If this

is done, a value of Q = 0.25 ± 0.05 or 0.65 ± 0.05 (δ< 0) is obtained for

the 1.389 Mev gamma transition. In summary, the results of the 1.389 Mev -

0.885 Mev and 0.885 Mev - 0.656 Mev correlations are consistent with spin

sequences of 5(D,Q)4(Q)2(Q)0, 6(0)3(D,Q)2(Q)0 and 4(D,Q)3(D,Q)2(Q)0.

A further check on the spins of levels IV and VI is provided by

the data for the 1.389 Mev - 0.656 Mev correlation. The 1.389 - 0.656

correlation is a 1-3 correlation with the intermediate radiation unobserved.

Even though the results of this correlation are ambiguous due to the inter-

fering cascades, it is most certain that the 1.389 - 0.656 correlation

possesses a fairly large negative asymmetry. The theoretical 1-3 correla-

tion function can be calculated for the possible sequences using equations

(12), (13) and (14) of Chapter I.

For a 5(D,Q)4(Q)2(Q)0 sequence, the theoretical 1-3 correlation

function is identical to the 5(D,Q)4(Q)2 correlation function. If this is

the correct spin sequence, the 1.389 - 0.656 correlation should be identical

to the 1.389 - 0.885 correlation. The experimental data tends to support

the $5(D,Q)4(Q)2(Q)0$ sequence since the 1.389 - 0.885 correlation shows

an asymmetry of 39% negative while the results of the 1.389 - 0.656 cor-

relation indicate an asymmetry of about 40% negative.

If the theoretical 1-3 correlation function for a $6(0)3(D,Q)2(Q)0$

sequence is calculated, the resulting coefficients are

$$A_2 = 0.179(1-Q) + 0.045 \ Q$$

$$A_4 = -0.0043(1-Q) + 0.0065 \ Q$$

where Q is the quadrupole content of the unobserved radiation. Inserting

the value of $Q = 0.09 \pm 0.02$ determined previously from the 1.389 - 0.885

and 0.885 - 0.656 correlation data, a value of $A_2 = 0.167 \pm 0.003$ is

found. (A_4 is negligible). This corresponds to an asymmetry of about

25% positive. Since the asymmetry of the 1.389 - 0.656 correlation is

certainly negative, the $6(0)3(D,Q)2(Q)0$ sequence for levels VI, IV, II

and I can be ruled out.

The theoretical 1-3 correlation function for a $4(D,Q)3(D,Q)2(Q)0$

sequence can likewise be calculated. The resulting coefficients are

$$A_2 = \left[0.1443(1-Q_1)+1.443 \sqrt{Q_1(1-Q_1)}+0.3093Q_1\right]\left[-0.4949(1-Q_2)-0.1237Q_2\right]$$

$$A_4 = 0.1489Q_1 \left[-0.4467(1-Q_2)+0.6701Q_2\right]$$

where Q_1 is the quadrupole content of the 4-3 transition and Q_2 is the

quadrupole content of the 3-2 transition. Inserting the values of $Q_1 =$

0.25 or 0.65 ($\delta < 0$) and $Q_2 = 0.04$ ($\delta < 0$) found previously from the 1.389 -

0.885 and 0.885 - 0.656 correlations, the results are $A_2 = 0.21$, $A_4 =$

0.015 for $Q_1 = 0.25$, and $A_2 = 0.21$, $A_4 = 0.039$ for $Q_1 = 0.65$. Both of

these sets of coefficients correspond to an asymmetry of about 33% posi-

tive, and since the 1.389 - 0.656 asymmetry is certainly negative, the

$4(D,Q)3(D,Q)2(Q)0$ spin sequence can be discarded.

Therefore the $5(D,Q)4(Q)2(Q)0$ sequence is the only sequence of spins for levels VI, IV, II and I which will simultaneously satisfy the results of the 1.389 Mev - 0.885 Mev, 0.885 Mev - 0.656 Mev, and 1.389 Mev - 0.656 Mev correlations. With this sequence, the correlation data requires the 1.389 Mev gamma transition to be a mixture of $(13.5 \pm 1.5)\%$ quadrupole and $(86.5 \mp 1.5)\%$ dipole radiation.

Because directional correlation results alone cannot determine the parity of the states involved, one must turn to other considerations if parities are to be assigned to levels IV and V. Since the spin and parity of the Ag^{110m} level are 6 and + respectively and the experimental evidence indicates that the 87 kev beta transition is an allowed transition, level VI must have positive parity. Therefore an assignment of 5^+ is made to level VI. The 1.389 Mev gamma transition consists of a mixture of 13% quadrupole and 87% dipole radiation according to the correlation results. An E1-M2 mixture of this magnitude is very unlikely, but an M1-E2 mixture is quite probable. Therefore an M1-E2 mixture is assumed for the 1.389 Mev transition, and the parity of level IV must then be positive. This requires the 0.885 kev gamma to be E2 radiation. The assignment of 4^+ to level IV is consistent with the fact that there is no observed beta transition from the Ag^{110m} level to this level. The beta transition would have to be second forbidden ($\Delta J = 2$, no; log ft $\sim$ 12-15) and therefore the transition probability could be small compared to the transition probabilities for the two observed betas. The 4^+ assignment is also consistent with the fact that in even-even nuclei, low-lying levels with even spin normally have even parity.

Interpretation of the 0.935 Mev - 0.885 Mev Correlation

Level V and the 0.935 Mev - 0.885 Mev correlation must now be

considered. The possible spins for level V are 4, 5, and 6. Since the spins of levels IV and II have already been established as 4 and 2 respectively, the combinations to be considered for the 0.935 Mev - 0.885 Mev correlation are 4-4-2, 5-4-2 and 6-4-2. In Figure 16 the theoretical curves for pure $6(Q)4(Q)2$ and $4(D)4(Q)2$ sequences are plotted together with the observed 0.935 Mev - 0.885 Mev correlation function. The theoretical coefficients for a $6(Q)4(Q)2$ sequence are $A_2 = 0.1020$ and $A_4 = 0.0091$, and for a $4(D)4(Q)2$ sequence they are $A_2 = 0.1965$ and $A_4 = 0$. The experimental values of the coefficients are $A_2 = 0.150 \pm 0.027$ and $A_4 = -0.006 \pm 0.036$. Neither of these sequences is quite consistent with the experimental data, but they are both close enough to warrant consideration as possibilities. They cannot be definitely discarded on the basis of the correlation data alone because the 0.935 - 0.885 correlation was obtained by a subtraction process which introduces uncertainties in the data. The other pure sequence which must be considered is $5(D)4(Q)2$. This possibility can be ruled out, however, since it would require a negative value for A_2.

If dipole-quadrupole mixtures are considered for the 0.935 Mev transition, both the $5(D,Q)4(Q)2$ and $4(D,Q)4(Q)2$ sequences are consistent with the 0.935 - 0.885 correlation data. In Figure 23 the theoretical values of A_2 and A_4 are plotted versus the quadrupole content of the 5-4 transition for a $5(D,Q)4(Q)2$ sequence. The experimental data are seen to be consistent with a value of $Q = 0.14 \pm 0.04$ ($\delta < 0$). A similar curve for the $4(D,Q)4(Q)2$ sequence is shown in Figure 24. For this case, the data are compatible with a value of $Q = 0.020 \pm 0.018$ ($\delta < 0$).

Since the background correlation determination was carefully done and a $\pm 10\%$ error assigned to the background before subtraction it
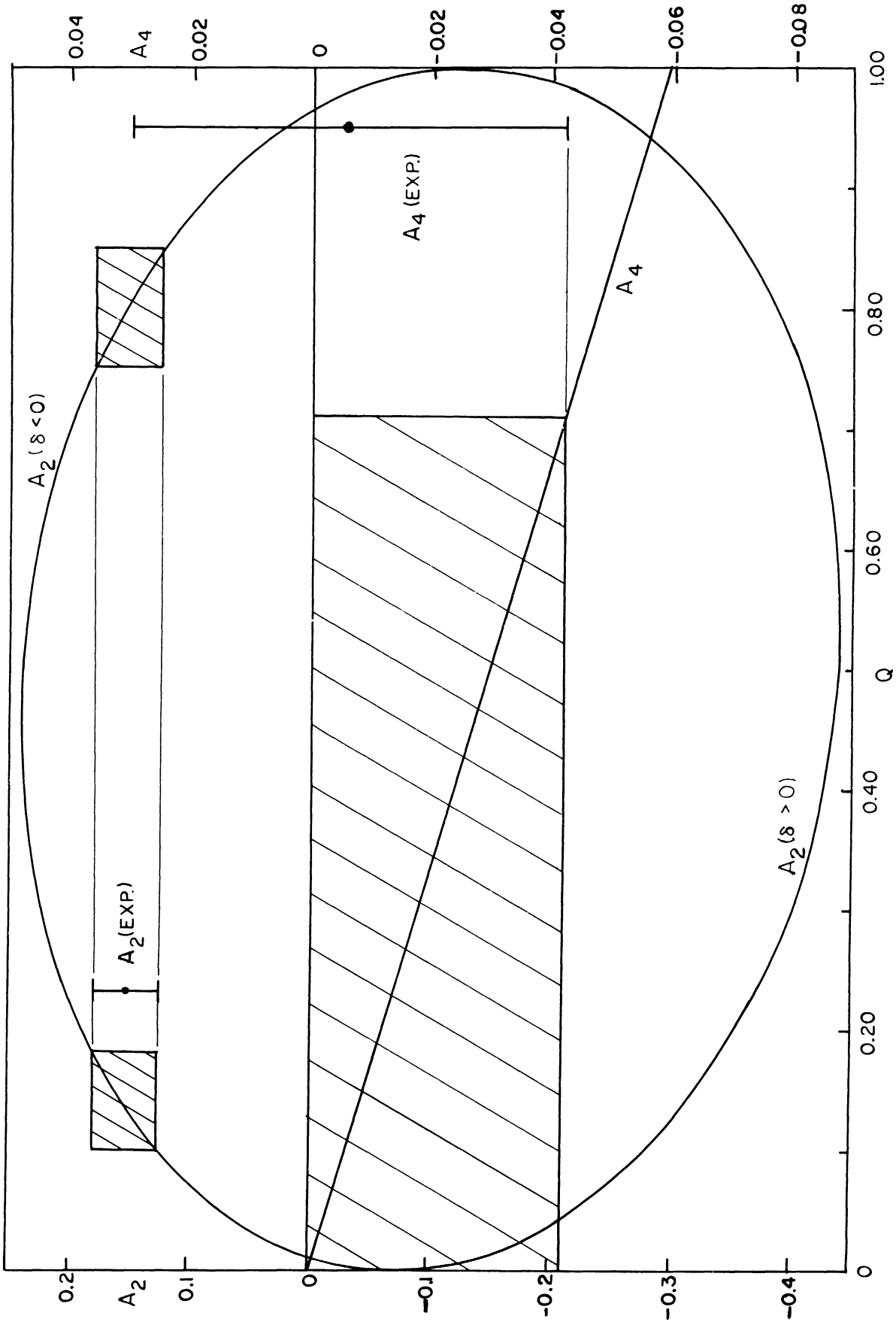
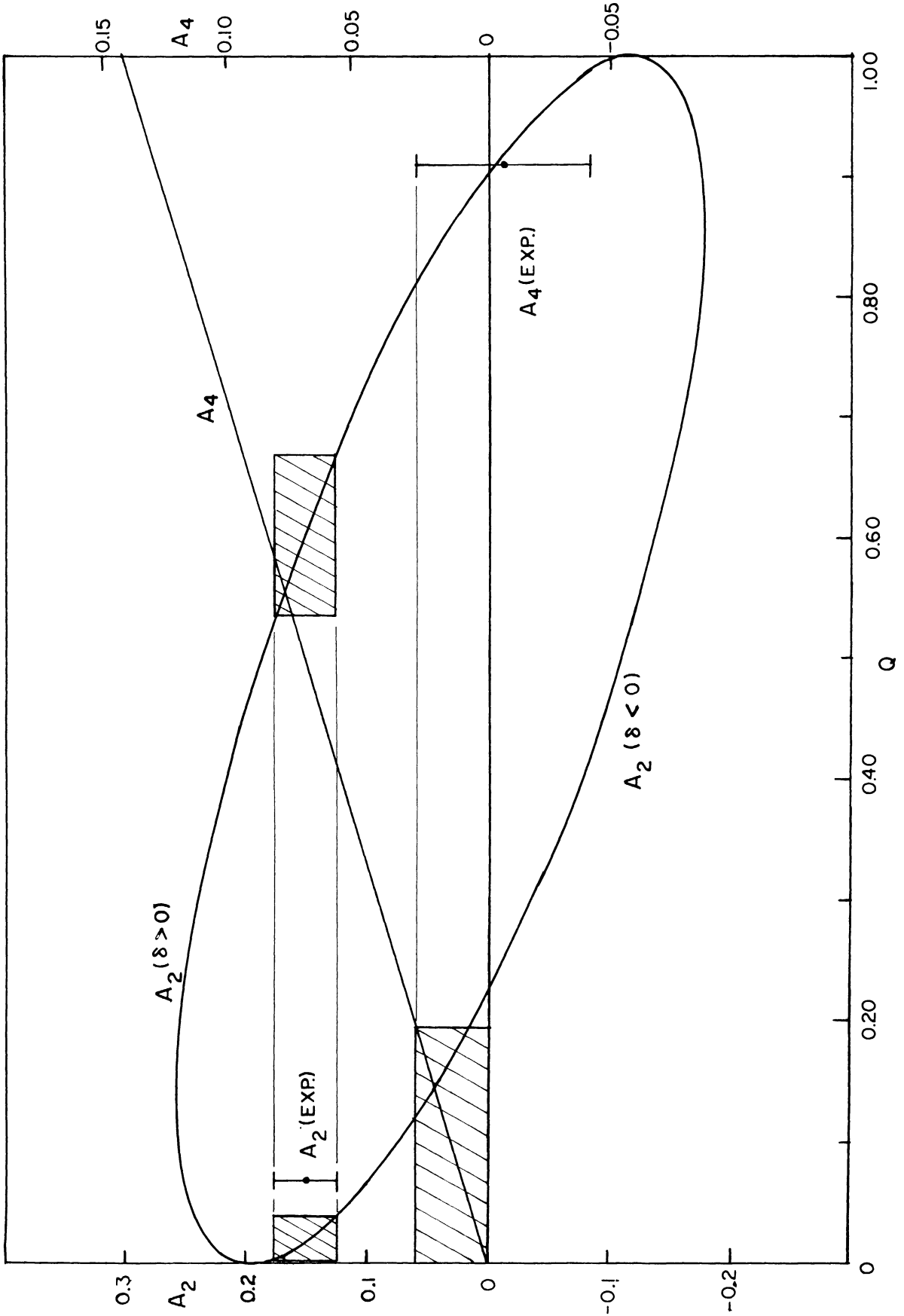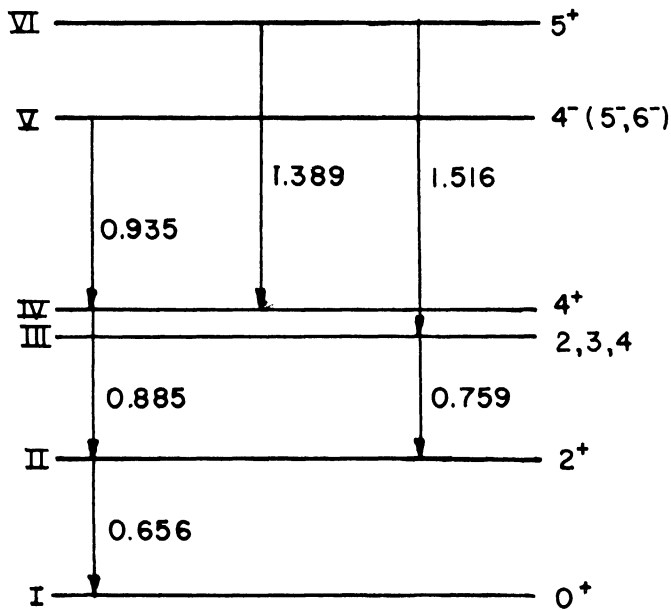Figure 23. A_2 and A_4 vs. Q for a $5(D,Q)4(Q)2$ Sequence

Figure 24. A_2 and A_4 vs Q for a $4(D,Q)4(Q)2$ Sequence

is believed that the data for the 0.935 - 0.885 correlation are accurate.
On this basis it is assumed that the 5(D,Q)4(Q)2 and 4(D,Q)4(Q)2 sequences
are more likely than the 4(D)4(Q)2 and 6(Q)4(Q)2 sequences, which were
not in good agreement with the experimental data. Thus the results of
the 0.935 Mev - 0.885 Mev correlation support a spin of 4 or 5 for level
V with the possibility of spin 6. If the spin is 4, the 935 kev transition
consists of a mixture of (98.0 $\pm$ 1.8)% dipole and (2.0 $\mp$ 1.8)% quadrupole
radiation. If the spin is 5, the 935 kev transition consists of a mix-
ture of (86 $\pm$ 4)% dipole and (14 $\mp$ 4)% quadrupole radiation.

Consider a spin of 5 for level V. Since an E1-M2 mixture of the
magnitude needed to explain the data is very unlikely it must be assumed
that the mixture is of M1-E2 character. This requires an assignment of
5^+ for level V, and therefore the 530 kev beta transition would have to
be of allowed type. However, this disagrees with the beta decay data which
indicates that this is a forbidden transition (log ft $\sim$ 8). On this basis
it is concluded that a spin of 5 for level V is not very likely. Consider
now a spin of 4. Since only a small admixture of quadrupole radiation
is indicated by the data, the argument against E1-M2 mixtures cannot be
used here. A value of 4^+ for level V would require the 530 kev beta to
be a second forbidden transition ($\Delta J = 2$, no; log ft $\sim$ 12-15) which dis-
agrees with the experimental log ft value of about 8. An assignment of
4^- for level V seems to agree best with the beta decay data and correlation
results. This requires a unique first forbidden beta transition ($\Delta J = 2$,
yes; log ft $\sim$ 7.5 - 9.5) and almost pure E1 radiation for the 0.935 Mev
gamma transition. The less likely possibility of spin 6 for level V would
require an assignment of 6^- and M2 radiation for the 0.935 Mev transition.

Therefore the correlation data for the 0.935 Mev - 0.885 Mev

cascade considered together with the beta decay data indicate a preference

for an assignment of 4⁻ to level V with assignments of 5⁻ and 6⁻ being

much less likely. The results up to this point are summarized in the

level scheme shown below.

```
VI ———————————————————————— 5⁺
                  │        │
V  ——————————————————————— 4⁻(5⁻,6⁻)
       │       1.389    1.516
     0.935     │        │
IV ——————————————————————— 4⁺
III———————————————————————— 2,3,4
     0.885            0.759
       │               │
II ——————————————————————— 2⁺
     0.656
       │
I  ——————————————————————— 0⁺
```

Interpretation of 1.516 Mev - 0.759 Mev and 1.516 Mev - 0.656 Mev Correlations

The 1.516 Mev - 0.759 Mev and 1.516 Mev - 0.656 Mev directional

correlations will now be considered. These are not too accurate but could

give some indication as to the spin of level III. According to the level

scheme, the 1.516 - 0.656 correlation is a 1-3 correlation while the

1.516 Mev - 0.759 Mev correlation is a simple 1-2 correlation. The se-

quences which must be considered for the 1.516 Mev - 0.656 Mev correlation

are $5(0)2(D,Q)2(Q)0$, $5(Q)3(D,Q)2(Q)0$ and $5(D,Q)4(Q)2(Q)0$. From the experi-

mental data it is certain that the 1.516 Mev - 0.656 Mev correlation must

have a large negative asymmetry. If the 1-3 correlation theoretical

values for A_2 and A_4 are calculated for the sequences $5(0)2(D,Q)2(Q)0$

and $5(Q)3(D,Q)2(Q)0$, it is found that neither sequence can give a negative asymmetry greater than 6%, no matter what the mixing parameter is. Therefore these sequences can be ruled out. If the spin sequence is $5(D,Q)4(Q)2(Q)0$, the 1-3 correlation function is identical to the 1-2 correlation. Thus the 1.516 - 0.656 and 1.516 - 0.759 correlations would have to be equal. The data shown in Table 3 are not in agreement with this, and any interference which might be present due to the highly negative 1.389 - 0.885 and 1.389 - 0.656 correlations cannot possibly explain the discrepancy.

Therefore the data for the 1.516 Mev - 0.656 Mev and 1.516 Mev - 0.759 Mev correlations are not in agreement with any of the possible spins 2, 3, or 4 for level III. It is of interest to consider the possibility of these two transitions occurring in the reverse order, thereby introducing a new Cd^{110} level at about 2.170 Mev and removing the level at 1.415 Mev (level III).

If the 1.516 Mev and 0.759 Mev transitions are reversed, the sequences which must be considered for the 1.516 Mev - 0.656 Mev correlation are $4(Q)2(Q)0$, $3(D,Q)2(Q)0$, and $2(D,Q)2(Q)0$. The $4(Q)2(Q)0$ sequence can be ruled out since it gives a positive value for A_2 and a positive asymmetry. The $2(D,Q)2(Q)0$ sequence can have an A_2 as large as -0.31 for a quadrupole content of 70%, but this mixture would require a large value for A_4 ($A_4 = +0.22$) which is inconsistent with the data. Furthermore, the $2(D,Q)2(Q)0$ sequence would require magnetic octopole radiation for the 0.759 Mev transition. This is very unlikely if one considers the relative intensities of the 0.759 Mev and 1.389 Mev transitions and the fact that the 1.389 Mev transition is primarily M1 radiation. Thus the $2(D,Q)2(Q)0$ sequence is discarded as a possibility. However, the $3(D,Q)2(Q)0$ sequence

will explain the data for the 1.516 Mev - 0.656 Mev correlation. Figure 25 shows the mixture curve for this sequence along with the experimental values of A_2 and A_4. From Figure 25 it is determined that the data are consistent with a value of Q between 0.11 and 0.97 ($\delta > 0$).

Therefore one should be able to explain the 1.516 Mev - 0.759 Mev correlation data by a $5(Q)3(D,Q)2$ sequence with a value of Q between 0.11 and 0.97 ($\delta > 0$). In Figure 26 the mixing curve for a $5(Q)3(D,Q)2$ sequence is shown. The experimental value of A_2 for the 1.516 - 0.759 correlation is indicated by the error flag. The data is consistent with a value of $Q = 0.07^{+0.15}_{-0.07}$ or $Q = 0.77^{+0.17}_{-0.20}$ but for $\delta < 0$. Consequently, the 1.516 - 0.759 correlation does not verify the results of the 1.516 - 0.656 correlation.

One can argue, however, that the interference from the highly negative 1.389 - 0.656 and 1.389 - 0.885 correlations and an inaccurate determination of the amount of 1.516 - 0.656 correlation present in the observed 1.516 - 0.759 correlation could cause the 1.516 - 0.759 result to be incorrect. These interference effects would all tend to make the 1.516 - 0.759 correlation more negative than it actually is. It is conceivable that the interference could even shift the asymmetry from a small positive value to a negative value. From Figure 26 it can be determined that a value of $A_2 = 0.06$ for the 1.516 - 0.759 correlation would be consistent with the lowest possible value for Q determined from the 1.516 - 0.656 data, namely $Q = 0.11$ ($\delta > 0$). A value of $A_2 = 0.06$ would correspond to an asymmetry of about 9% positive (if A_4 is negligible). The smallest value for the observed asymmetry of the 1.516 - 0.759 correlation, considering the experimental error, is about 9% negative. Therefore, if it is conceded that the interference effects could shift the asymmetry from
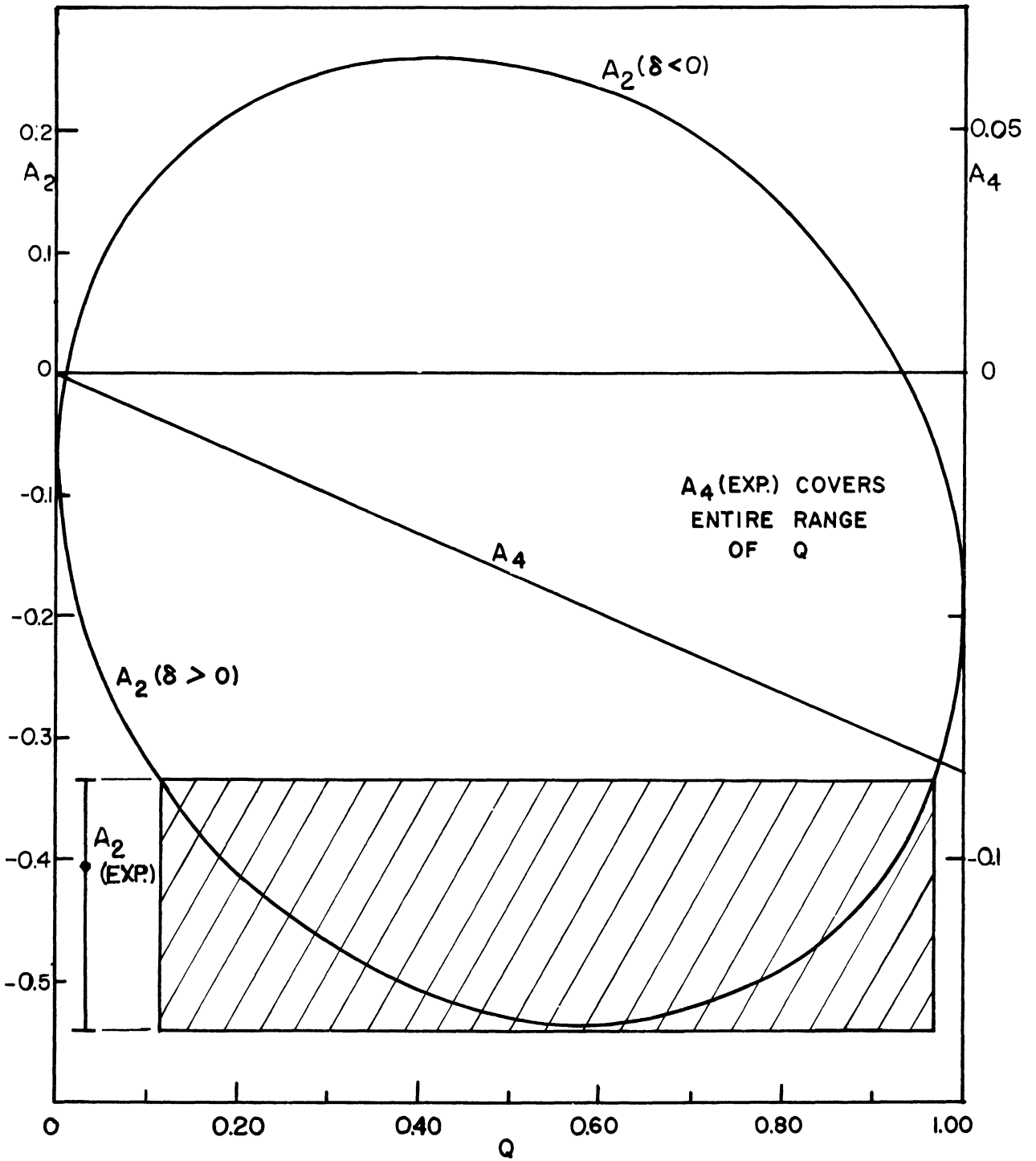
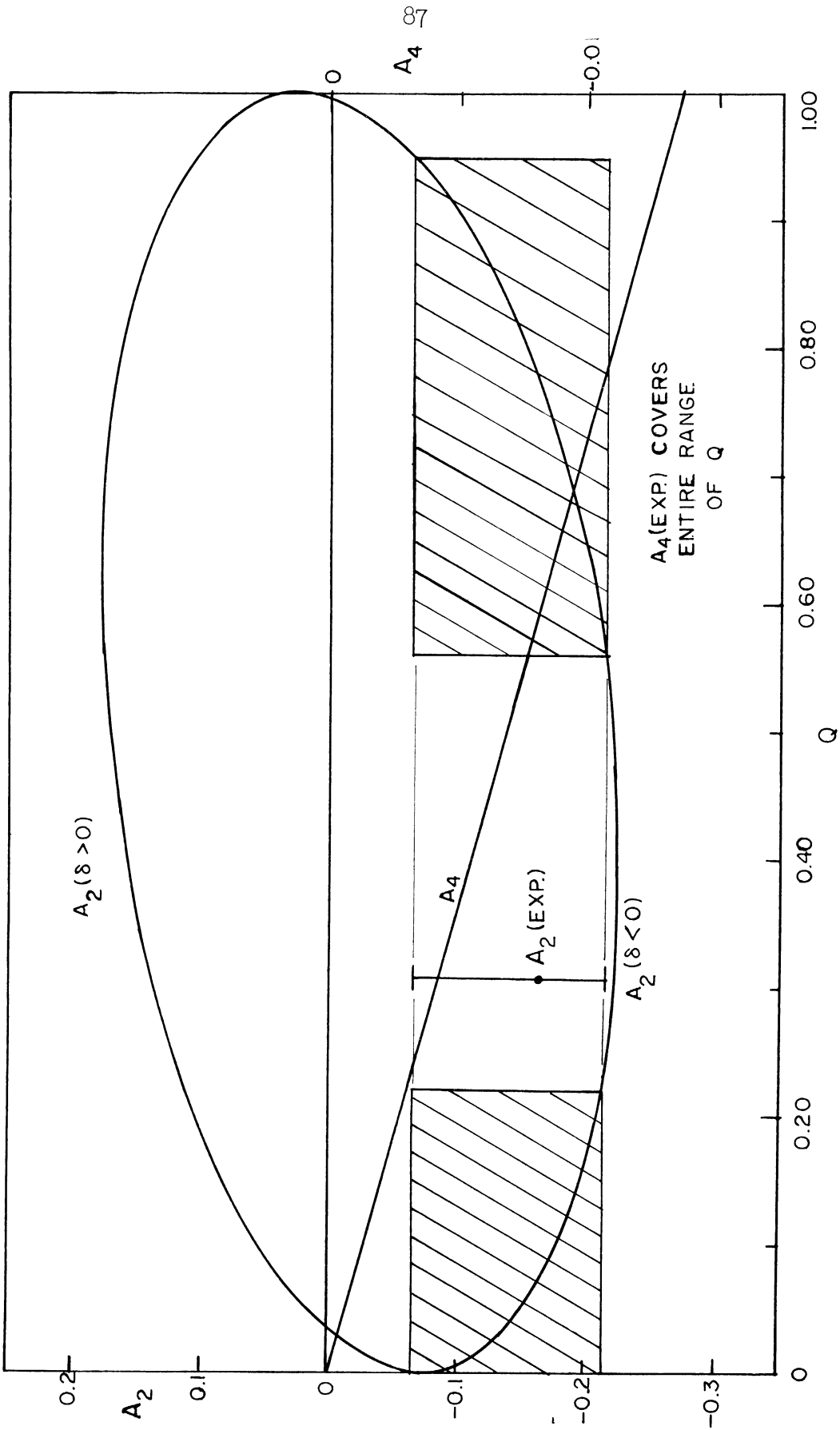Figure 25. A_2 and A_4 vs. Q for a 3(D,Q)2(Q)0 Sequence.

Figure 26. A2 and A4 vs. Q for a 5(Q)3(D,Q)2 Sequence

9% positive to 9% negative, the 5(Q)3(D,Q)2(Q)0 sequence will explain

both the 1.516 Mev - 0.656 Mev and 1.516 Mev - 0.759 Mev correlations.

Because the results of these correlations are so inaccurate and

the interpretation so vague it is difficult to make a conclusion as to

whether the 1.516 kev transition precedes or follows the 0.759 transition.

However, the data is more nearly consistent with the sequence in which

the 0.759 Mev transition precedes the 1.516 Mev transition, and on this

basis it is felt that this is the correct order. This requires a new

Cd^{110} level at 2.170 Mev and removes the level at 1.415 Mev. If this

new level is actually present, it most certainly has a spin of 3 and

probably positive parity as indicated by the correlation data.

It was stated previously that several of the weak gamma transi-

tions found in Cd^{110} would not fit into the accepted decay scheme shown

in Figure 13. However, if one considers the new level order suggested

by the correlation measurements, all of the gamma transitions reported

by Antoneva, et al.[71] can be arranged in a consistent level scheme.

This scheme is shown in Figure 27. The transition energies and beta

branching ratios are those reported by Antoneva[71] and differ slightly

from the values found by Siegbahn[70]. The spin and parity values listed

for the Cd^{110} levels are those found in the present investigation. The

new decay scheme retains the same positioning of the 0.655 Mev, 0.883 Mev,

0.932 Mev, and 1.386 Mev transitions as the former scheme, and therefore

none of the correlation measurements are affected by the change. The

fact that all of the transitions can be arranged in a consistent scheme

gives strong support to the conclusion that the 0.759 Mev gamma ray pre-

cedes the 1.506 Mev gamma ray. Further discussion of this new level
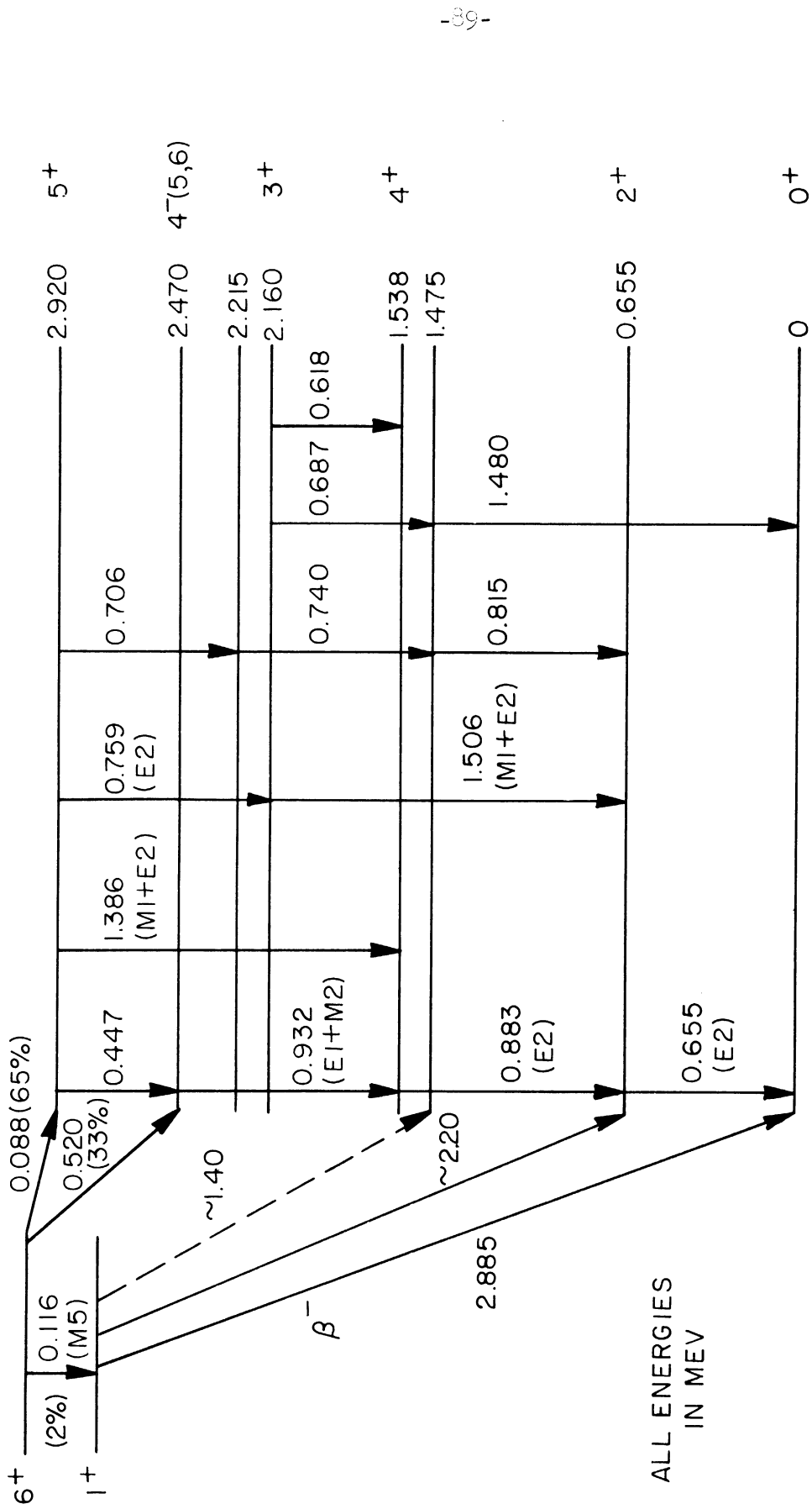
scheme will be presented in the next section.

Figure 27. Revised Level Scheme for Cd^{110}

Summary and Discussion

The directional correlation data for Cd^{110} presented in the previous sections is in good agreement with the assignment of 0^+, 2^+, 4^+ and 5^+ for the ground state, 0.655 Mev level, 1.538 Mev level, and 2.920 Mev level respectively. The data indicate a preference for an assignment of 4^- to the 2.470 Mev level, but spins of 5 and 6 are also possible. The assignments for these levels are supported by the beta decay data[70,71] and internal conversion coefficient measurements[70]. The correlation results indicate that the 0.759 Mev gamma transition precedes the 1.506 Mev gamma transition, rather than being in the opposite order previously reported[70]. Additional evidence for this positioning of the 1.506 Mev and 0.759 Mev transitions is provided by the fact that all of the gamma transitions reported by Antoneva, et al.[71], can be placed in a consistent level scheme. This scheme requires new levels at about 1.475 Mev and 2.160 Mev. If this new scheme is correct, the correlation data indicate a spin of 3 and probably positive parity for the 2.160 Mev level. Figure 27 shows the revised decay scheme. The spin and parity assignments made in the present investigation are listed beside the appropriate Cd^{110} levels. With these assignments, the 0.655 Mev, 0.759 Mev and 0.885 Mev transitions are pure E2 radiation, the 1.386 Mev transition is a mixture of $(86.5 \pm 1.5)\%$ M1 and $(13.5 \mp 1.5)\%$ E2 radiation, the 0.932 Mev transition is a mixture of $(98.0 \pm 1.8)\%$ E1 and $(2.0 \mp 1.8)\%$ M2 radiation, and the 1.506 Mev transition is a mixture of M1 and E2 radiation (degree of mixture uncertain).

According to the revised decay scheme, the second excited state has an energy of about 1.475 Mev, and a weak cross-over transition occurs from this state to the ground state. This would be consistent with a

spin value of 2^+ for the 1.475 Mev level. Therefore one might expect a weak beta transition of about 1.40 Mev occurring between the 1^+ Ag^{110} level and the 1.475 Mev Cd^{110} level. There is actually some evidence for this beta transition, because Antoneva[71] had reported the possibility of a beta transition with end-point energy of just about 1.40 Mev (dotted line in Figure 27).

Since the Cd^{110} nucleus consists of 48 protons (closed shell minus 2) and 62 neutrons (closed shell plus 12), it might be expected that Cd^{110} would exhibit some vibrational level structure. The ratio of the energies of the second and first excited states is 2.25 according to the new level scheme, and the 1.480 Mev cross-over transition is much weaker than the 0.815 Mev transition. If the spin of the 1.475 Mev level is 2^+, then both of these results suggest that the first two excited states are probably the result of vibrational excitations. Additional evidence for vibrational level structure is provided by the Coulomb excitation results for Cd^{110}, which show that the cross-section for Coulomb excitation of the first excited state is larger than that expected for a single par-ticle excitation[65,78,79].

If the new level scheme is considered, the relative intensities of the gamma transitions can be explained quite satisfactorily by the spin, parity, and multipole assignments which were made on the basis of the correlation results. The fact that the transitions occurring from the second excited state are much weaker than those occurring from the third excited state is plausible if one considers the manner in which the 1.475 Mev level is fed. If the spin of this level is 2^+ as indicated, a direct transition from the 2.920 Mev state (5^+) would require M3 radi-ation, and this transition could not compete with the 0.759 Mev (E2) and

1.386 Mev (M1 + E2) transitions. A direct transition from the 2.470 Mev

level (4⁻) to the 1.475 Mev level would require M2 radiation, and this

transition could not compete with the 0.932 Mev gamma which is almost

pure E1 radiation. Moreover, a transition from the 1.538 Mev level (4⁺)

to the 1.475 Mev level would require E2 radiation and could not compete

with the 0.883 Mev (E2) transition because of the large transition energy

difference. The observed gamma rays which feed the second excited state

are the 0.740 Mev and 0.687 Mev transitions. These are weak due to the

competition from the higher energy gamma rays of comparable multipole

order. Therefore if one considers the spins shown in Figure 27, the small

intensities for the 0.815 Mev and 1.480 Mev gamma transitions relative

to the 0.883 Mev gamma intensity can be explained.

If the spin assignments for the 2.470 Mev and 0.655 Mev levels

are 4⁻ and 2⁺ as indicated in Figure 27, one might expect an M2 gamma

transition of 1.815 Mev occurring between these levels. Some evidence for

a weak transition of this energy has been found by Dzelepov[83]. However,

he reported that the existence of this gamma ray was questionable.

Because of the success in fitting all of the gamma transitions

into this new level scheme and the apparent explanation of the intensities

in terms of the spin, parity, and multipole assignments indicated by the

correlation measurements, it is reasonable to conclude that this is the

correct level scheme and that the assignments for the Cd^{110} levels are

correct. Moreover, it is apparent that the first and second excited states

in Cd^{110} are mainly due to vibrational excitations and that the spin of

the second excited state is probably 2⁺.

BIBLIOGRAPHY

1. Arfken, Biedenharn and Rose, Phys. Rev., 84, 89 (1951).

2. Brady, E. L. and Deutsch, M., Phys. Rev., 78, 558 (1950).

3. Stevenson, D. T. and Deutsch, M., Phys. Rev., 78, 640 (1950).

4. Beling, Feld and Halpern, Phys. Rev., 84, 155 (1951).

5. McGowan, F. K., Phys. Rev., 92, 524 (1953).

6. Dunworth, J. W., Rev. Sci. Instr., 11, 167 (1940).

7. Hamilton, D. R., Phys. Rev., 58, 122 (1940).

8. Goertzel, G., Phys. Rev., 70, 897 (1946).

9. Brady, E. L. and Deutsch, M., Phys. Rev., 72, 870 (1947).

10. Brady, E. L. and Deutsch, M., Phys. Rev., 74, 1541 (1948).

11. Falkoff, D. L., Doctoral Thesis, University of Michigan (1948).

12. Falkoff, D. L. and Uhlenbeck, G. E., Phys. Rev., 79, 323 (1950).

13. Gardner, J. W., Proc. Phys. Soc. London, A62, 763 (1949).

14. Ling, D. S. and Falkoff, D. L., Phys. Rev., 76, 1639 (1949).

15. Racah, G., Phys. Rev., 84, 910 (1951).

16. Fano, U., Phys. Rev., 90, 577 (1953).

17. Fano, U., National Bureau of Standards Report 1214.

18. Lloyd, S. P., Phys. Rev., 85, 904 (1952).

19. Alder, K., Helv. Phys. Acta, 25, 235 (1952).

20. Coester, F. and Jauch, J., Helv. Phys. Acta, 26, 3 (1953).

21. Frauenfelder, H., Beta and Gamma Ray Spectroscopy, North-Holland Publishing Co., 1955.

22. Blatt, J. M. and Weisskopf, V. F., Theoretical Nuclear Physics, John Wiley and Sons, 1952.

23. Deutsch, M., Report Phys. Soc. Prog. Phys., 14, 196 (1951).

24. Ling, D. S. and Falkoff, D. L., Phys. Rev., 76, 1639 (1949).

25. Eckart, C., Revs. Modern Phys., 2, 305 (1930).

26. Wigner, E. P., _Gruppentheorie_, F. Vieweg and Sohn, Braunschweig, 1931.

27. Heitler, W., _Quantum Theory of Radiation_, Oxford Univ. Press, 1944, 1954 .

28. Moszkowski, S. A., _Beta and Gamma Ray Spectroscopy_, North-Holland Publishing Co., 1955 .

29. Abragam, A. and Pound, R. V., _Phys. Rev._, 89, 1306 (1953).

30. Pound, R. V. and Abragam, A., _Phys. Rev._, 90, 993 (1953).

31. Abragam, A. and Pound, R. V., _Phys. Rev._, 92, 943 (1953).

32. Coester, F., _Phys. Rev._, 93, 1304 (1954).

33. Ferentz, H. and Rosenzweig, N., Argonne Natl. Lab. Report 5324 (1954)

34. Biedenharn, Arfken and Rose, _Phys. Rev._, 83, 586 (1951).

35. Arfken, Biedenharn and Rose, _Phys. Rev._, 86, 761 (1952).

36. Birks, J. B., _Scintillation Counters_, McGraw-Hill Book Co., 1953.

37. Schiff, L. I., _Phys. Rev._, 50, 88 (1936).

38. Stewart, M. G., Doctoral Thesis, University of Michigan (1955).

39. Frankel, S., _Phys. Rev._, 83, 673 (1951).

40. Church, E. L. and Kraushaar, J. J., _Phys. Rev._, 88, 419 (1952).

41. Rose, M. E., _Phys. Rev._, 91, 610 (1953).

42. Lawson, Jr., J. L. and Frauenfelder, H., _Phys. Rev._, 91, 649 (1953).

43. Private Communication from Arns, R. G.

44. Feingold, A. M. and Frankel, S., _Phys. Rev._, 97, 1025 (1955).

45. Walter, Huber and Zunti, _Helv. Phys. Acta_, 23, 697 (1950).

46. Stewart, M. G., Doctoral Thesis, University of Michigan (1955).

47. Scharenberg, R. P., Doctoral Thesis, University of Michigan (1955).

48. Elmore, W. C. and Sands, M., _Electronics_, McGraw-Hill Book Co., 1949.

49. Garwin, R. L., _Rev. Sci. Instr._, 21, 569 (1950).

50. Garwin, R. L., _Rev. Sci. Instr._, 24, 618 (1953).

51. Lu, D. C., Doctoral Thesis, University of Michigan (1954).

52. Rose, M. E., _Phys. Rev._, 91, 610 (1953).

53. Siegbahn, K., Arkiv Mat. Astron. Fysik, 34A, 1 (1947).

54. Hubert, P., J. Phys. radium, 12, 823 (1951).

55. Hubert, P., Ann. phys., 8, 662 (1953).

56. Kraushaar, J. J. and Goldhaber, M., Phys. Rev., 89, 1081 (1953).

57. Kurbatov, Murray and Sakai, Phys. Rev., 98, 674 (1955).

58. Pipkin, F. M. and Culvahouse, J. W., Phys. Rev., 106, 1102 (1957).

59. Nordheim, L. A., Revs. Modern Phys., 23, 322 (1951).

60. Metzger, F. R. and Todd, W. B., J. Franklin Inst., 256, 277 (1953).

61. Wiedling, T., Directional Correlation Measurements and Some Other
     Related Investigations of Excited Nuclei, Almquist and Wiksells
     Boktryckeri AB, Uppsala, 1956).

62. Coleman, C. F., Phil. Mag., 46, 1135 (1955).

63. Lindqvist, T. and Marklund, I., Nuclear Phys., 4, 189 (1957).

64. Rose, M. E., Multipole Fields, Wiley and Sons, 1955.

65. Alder, Bohr, Huus, Mottelson and Winther, Revs. Modern Phys., 28,
     432 (1956).

66. Moszkowski, S. A., Handbuch der Physik, 39, Springer-Verlag, Berlin,
     1957.

67. Wilets, L. and Jean, M., Phys. Rev., 102, 788 (1956).

68. Temmer, G. M. and Heydenburg, N. P., Phys. Rev., 104, 967 (1956).

69. Geiger, K. W., Phys. Rev., 105, 1539 (1957).

70. Siegbahn, K., Phys. Rev., 77, 233 (1950).

71. Antoneva, N. M., et al., Doklady Akad. Nauk SSSR, 77, 41 (1951).

72. Shpinel, V. S. and Forafontov, N. V., Zhur. Eksptl. i Teoret. Fiz,
     21, 1376 (1951).

73. Dzelepov, B. S., Doklady Akad. Nauk. SSSR, 77, 597 (1951).

74. Johansson, S. A. E. and Almquist, S., Arkiv Fysik, 5, 427 (1952).

75. Azuma, T., Phys. Rev., 94, 638 (1954).

76. Thomas, Jr., Whitaker and Peacock, Bull. Am. Phys. Soc., 1, No. 2,
     86, (1956).

77. Sliv, L. A. and Band, I. M., *Coefficients of Internal Conversion of Gamma Radiation.* Part 1, K-Shell, Leningrad Physico-Technical Inst., 1956

78. Temmer, G. M. and Heydenburg, N. P., *Phys. Rev.*, 104, 967 (1956).

79. Stelson, P. H. and McGowan, F. K., ORNL-2076, 6 (1956).

80. Mayer, M. G. and Jensen, J. H., *Elementary Theory of Nuclear Shell Structure*, Wiley and Sons, 1955.

81. Moszkowski, S. A., *Phys. Rev.*, 82, 35 (1951).

82. Ewbank, Nierenberg, Shugart, and Silsbee, *Bull. Am. Phys. Soc.*, 2, No. 6, (1957).

83. Dzelepov, B. S., *Proc. Acad. of Science of USSR, Physics Series (Izvestia)*, 20, 343 (1956).